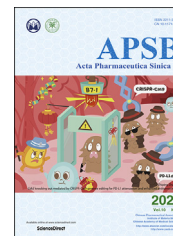




Chinese Pharmaceutical Association
Institute of Materia Medica, Chinese Academy of Medical Sciences

Acta Pharmaceutica Sinica B

www.elsevier.com/locate/apsb
www.sciencedirect.com



ORIGINAL ARTICLE

Nobiletin and its derivatives overcome multidrug resistance (MDR) in cancer: total synthesis and discovery of potent MDR reversal agents



Senling Feng^{a,†}, Huifang Zhou^{b,†}, Deyan Wu^b, Dechong Zheng^a,
Biao Qu^a, Ruiming Liu^a, Chen Zhang^b, Zhe Li^b, Ying Xie^{a,*},
Hai-Bin Luo^{b,*}

^aSchool of Pharmacy, State Key Laboratory for Quality Research in Chinese Medicines, Macau University of Science and Technology, Avenida Wai Long, Taipa, Macau, China

^bSchool of Pharmaceutical Sciences, Sun Yat-Sen University, Guangzhou 510006, China

Received 7 April 2019; received in revised form 5 July 2019; accepted 6 July 2019

KEY WORDS

Nobiletin;
Cancer multidrug
resistance;
Mechanism;
Nobiletin;
P-gp inhibition;
Reversal agents;
Solubility;

Abstract Our recent studies demonstrated that the natural product nobiletin (NOB) served as a promising multidrug resistance (MDR) reversal agent and improved the effectiveness of cancer chemotherapy *in vitro*. However, low aqueous solubility and difficulty in total synthesis limited its application as a therapeutic agent. To tackle these challenges, NOB was synthesized in a high yield by a concise route of six steps and fourteen derivatives were synthesized with remarkable solubility and efficacy. All the compounds showed improved sensitivity to paclitaxel (PTX) in P-glycoprotein (P-gp) overexpressing MDR cancer cells. Among them, compound **29d** exhibited water solubility 280-fold higher than NOB. A drug-resistance A549/T xenograft model showed that **29d**, at a dose of 50 mg/kg co-administered with PTX (15 mg/kg), inhibited tumor growth more effectively than NOB and remarkably increased PTX

Abbreviations: Ac₂O, acetic anhydride; AcOH, acetic acid; AcONa, sodium acetate; BF₃·Et₂O, boron trifluoride diethyl etherate; DCM, dichloromethane; DCE, dichloroethane; DMF, *N,N*-dimethylformamide; DMSO, dimethyl sulfoxide; DOX, doxorubicin; Et₃N, triethylamine; Flutax-2, a fluorescent taxol derivative; MDR, multidrug resistance; NOB, nobiletin; NIS, *N*-iodosuccinimide; P-gp, P-glycoprotein; PI, propidium iodide; PTX, paclitaxel; QND, quinidine; Rho123, rhodamine 123; *t*-BuOK, potassium *tert*-butylate; TCA, trichloroacetic acid; THF, tetrahydrofuran; TLC, thin-layer chromatography; SRB, sulforhodamine B; Ver, verapamil.

*Corresponding authors. Tel./fax: +86 20 39943000.

E-mail addresses: yxie@must.edu.mo (Ying Xie), luohb77@mail.sysu.edu.cn (Hai-Bin Luo).

†These authors made equal contributions to this work.

Peer review under responsibility of Institute of Materia Medica, Chinese Academy of Medical Sciences and Chinese Pharmaceutical Association.

<https://doi.org/10.1016/j.apsb.2019.07.007>

2211-3835 © 2020 Chinese Pharmaceutical Association and Institute of Materia Medica, Chinese Academy of Medical Sciences. Production and hosting by Elsevier B.V. This is an open access article under the CC BY-NC-ND license (<http://creativecommons.org/licenses/by-nc-nd/4.0/>).

Total synthesis

concentration in the tumors *via* P-gp inhibition. Moreover, Western blot experiments revealed that **29d** inhibited expression of NRF2, phosphorylated ERK and AKT in MDR cancer cells, thus implying **29d** of multiple mechanisms to reverse MDR in lung cancer.

© 2020 Chinese Pharmaceutical Association and Institute of Materia Medica, Chinese Academy of Medical Sciences. Production and hosting by Elsevier B.V. This is an open access article under the CC BY-NC-ND license (<http://creativecommons.org/licenses/by-nc-nd/4.0/>).

1. Introduction

As the second leading cause of death next to heart disease, cancer is a growing global threat with 18 million cases and 9.6 million deaths in 2018 around the world¹. Chemotherapy is commonly used for treatment of many types of cancers, but multidrug resistance (MDR) often causes chemotherapy failure, leading to death of a majority of patients². Overcoming drug resistance has far-reaching implications for cancer patients and society³. Cellular mechanisms of drug resistance have been classified into transport-based classical and nonclassical MDR phenotypes³. Overexpression of P-glycoprotein (P-gp, P-gp/ABCB1 encoded by the *MDR1* gene), one of the ABC-family efflux transporters, is associated with poor prognosis in many types of cancers and is frequently observed in recurrent tumors in clinic⁴. In the past 20 years, three generations of MDR inhibitors have been developed to target efflux transporters, especially P-gp. Unfortunately, drawbacks of the targeted therapy occurred after treatment for long time⁴. Recently, studies on reversal of MDR by natural products and their synthesized analogues, such as secalonic acid D, epigallocatechin gallate derivative, WS-10, etc^{5–7}, have received increasing attention. Among them, several fragments (Murcko, Murcko generic, RECAP and aromatic ring) are found to actively inhibit ABCB1⁶, serving as templates for designing new potent reversal agents to overcome MDR of cancers.

As a polymethoxy flavonoid isolated from tangerines, nobiletin (NOB, 3',4',5,6,7,8,-hexamethoxyflavone, Fig. 1) exhibits a good safety profile and a broad spectrum of pharmacological activities, such as anti-oxidative, anti-inflammatory⁸ and anti-tumor effects⁹, especially high potency in cocktail therapy for drug-resistant cancers¹⁰. However, NOB exists as an aglycone, has poor water solubility (1–5 µg/mL) and low oral bioavailability (<1%), which limit its application as a therapeutic agent¹¹. In addition to the traditional methods of separation and extraction, NOB could be prepared by total synthesis of over eleven steps¹². Our recent studies demonstrated that NOB worked as an inhibitor of the MDR-efflux proteins by competing with chemotherapy drugs for the same binding site of P-gp, thus leading to improvement of the effectiveness of cancer chemotherapy *in vitro*¹⁰. NOB showed the

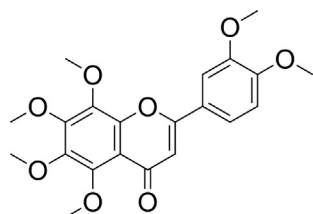


Figure 1 Chemical structure of nobiletin (NOB).

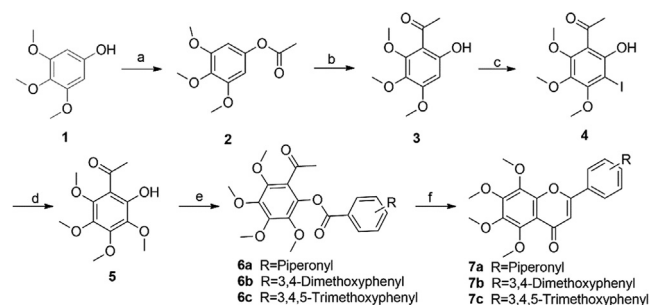
MDR reversal ability to make the ovarian tumor cells of A2780/T, which resisted to paclitaxel (PTX), became >400 folds sensitive in comparison with its parent A2780 cells. Although there are lots of synthesized compounds or natural products demonstrated for their MDR reversal abilities, few of them have comparable reversal ability with NOB. In addition, our previous study revealed that NOB not only inhibited the P-gp function but also modulated the NRF2/PI3K/AKT pathways which are the important mechanisms of the MDR. These findings encourage further studies on producing NOB and its derivatives in a simpler and more effective synthetic way to find more potent and soluble products.

Herein, to overcome the disadvantages and expand the scope of application, NOB was newly generated in high yield by a concise route of six steps and fourteen derivatives with remarkable solubility were synthesized. Further, we analyzed the efficacy of the compounds as MDR reversal agents in P-gp-overexpressing MDR cancer cells *in vitro* and in an A549/T xenograft model *in vivo*. We also investigated the underlying mechanism for the MDR reversal effects of NOB and its derivatives.

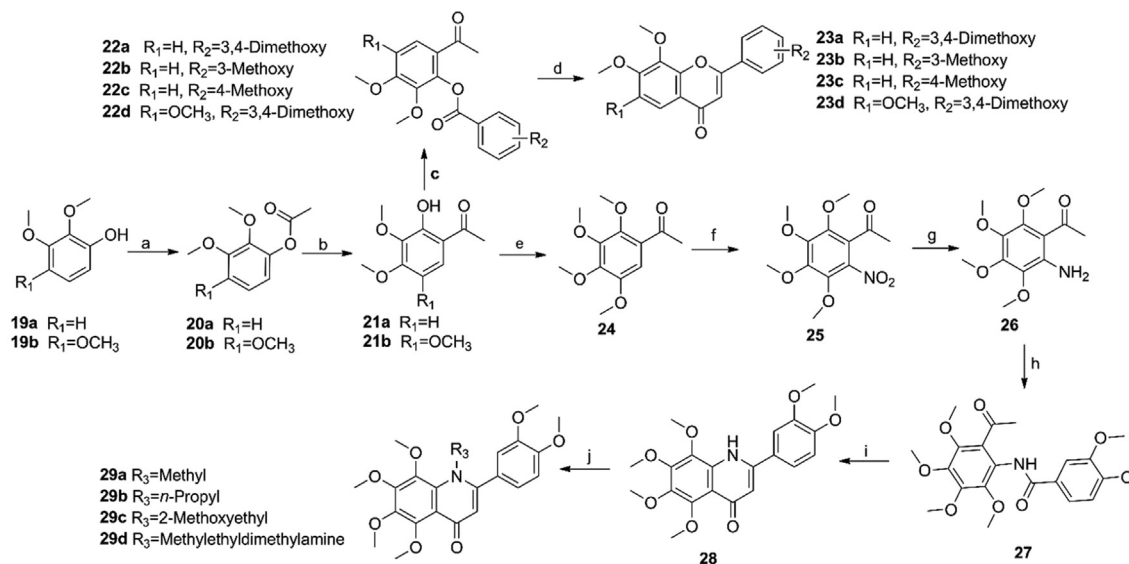
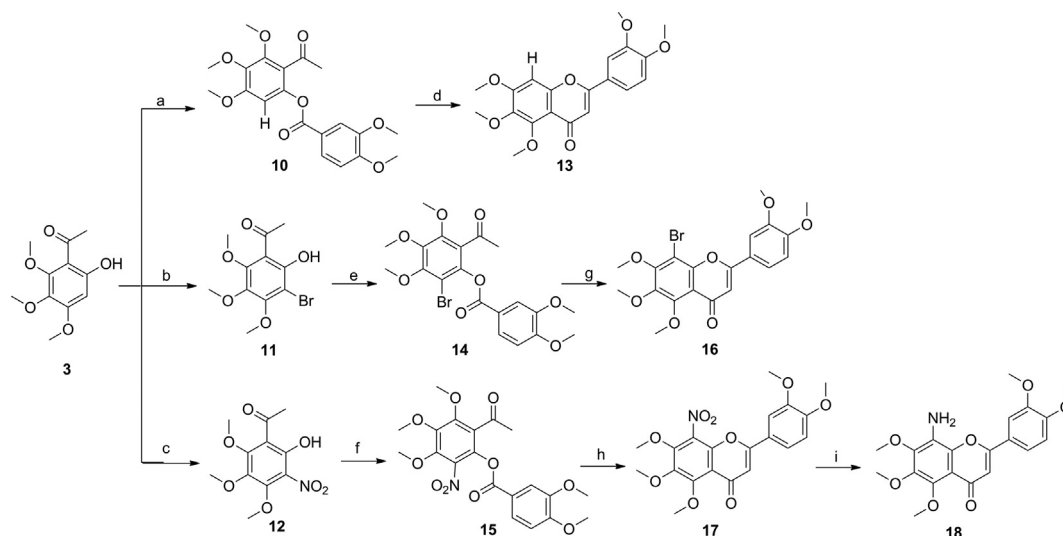
2. Results and discussion

2.1. Synthesis of the designed compounds

The target compounds were prepared by the synthetic routes reported in Schemes 1–3. First, commercially available 3,4,5-trimethoxyphenol (**1**) was selected as the starting material and reacted with acetic anhydride to afford the acetylation product **2**, followed by Fries rearrangement to provide **3**, which was then halogenated with *N*-iodosuccinimide to obtain



Scheme 1 Syntheses of 5,6,7,8-tetramethoxy-2-phenyl-4H-chromen-4-ones **7a–7c**. Reagents and conditions: (a) Ac₂O, AcOH, 110 °C, 2 h; (b) BF₃·Et₂O, AcOH, 70 °C, 2 h; (c) NIS, *p*-toluenesulfonic acid monohydrate, CH₃CN, rt, 2 h; (d) 4 mol/L MeONa in MeOH, CuCl, DMF, 90 °C, 30 min; (e) acyl chlorides, Et₃N, DCM, 0 °C to rt, 2 h; (f) triethylsilyl trifluoromethanesulfonate, Et₃N, DCE, reflux, 2 h.



Scheme 3 Syntheses of 2-(3,4-dimethoxyphenyl)-6,7,8-trimethoxy-4*H*-chromen-4-ones **23** and **29a–29d**. Reagents and conditions: (a) Ac₂O, AcOH, 110 °C, 2 h; (b) BF₃·Et₂O, AcOH, 70 °C, 2 h; (c) 3,4-dimethoxybenzoyl chloride, Et₃N, DCE, 0 °C to rt, 2 h; (d) triethylsilyl trifluoromethanesulfonate, Et₃N, DCE, reflux, 2 h. (e) iodomethane, K₂CO₃, DMF, rt, 1 h; (f) HNO₃, 0 °C, 10 min; (g) Pd/C, H₂, THF, rt, 12 h; (h) 3,4-dimethoxybenzoyl chloride, Et₃N, DCM, 0 °C to rt 2 h; (i) *t*-BuOK, THF, reflux, 12 h; (j) iodomethane, K₂CO₃, DMF, chloroalkanes, NaH, DMF, 90 °C, 2.5 h.

compound **4** (Scheme 1). The key intermediate 1-(2-hydroxy-3,4,5,6-tetramethoxyphenyl)ethan-1-one (**5**) was synthesized by the reaction of **4** with sodium methoxide in the presence of copper chloride¹³. Compounds **6a–6c** were synthesized by acylation of **5** with the corresponding acyl chlorides¹⁴. The target compounds **7a–7c** were obtained by cyclization of **6a–6c** in the presence of triethylsilyl trifluoromethanesulfonate, respectively.

As outlined in Scheme 2, compounds **11** and **12** were obtained from **3** by treatment with bromine and nitric acid, respectively. Aryl

esters **10**, **14** and **15** were synthesized by acylation of 1-(2-hydroxyphenyl)ethan-1-ones with the corresponding acyl chlorides, which were treated with triethylsilyl trifluoromethanesulfonate to provide the corresponding flavones **13**, **16** and **17**. Subsequently, compound **17** was reduced by catalytic hydrogenation with Pd/C to afford 8-amino-2-(3,4-dimethoxyphenyl)-5,6,7-trimethoxy-4*H*-chromen-4-one (**18**).

Furthermore, commercially available 2,3-dimethoxyphenol (**19a**) or 2,3,4-trimethoxyphenol (**19b**) were selected as the

starting materials, and the same procedures as in Schemes 1 and 2 were used to obtain compounds **23a–23d** (Scheme 3). The intermediate **21b** was treated with iodomethane and K_2CO_3 in the presence of *N,N*-dimethylformamide (DMF) to obtain **24**, followed with nitric acid to afford compound **25**. After **25** was reduced by catalytic hydrogenation with Pd/C to yield compound **26**, it was treated with 3,4-dimethoxybenzoyl chloride to obtain **27**. Finally, **27** was treated with *t*-BuOK in a solution of tetrahydrofuran (THF) to produce 2-(3,4-dimethoxyphenyl)-5,6,7,8-tetramethoxyquinolin-4(1*H*)-one (**28**)¹⁵. Compounds **29a–29d** were synthesized by the reaction of **28** and corresponding alkyl halides in the presence of sodium hydride.

To avoid the interference of false positive compounds in our subsequent study, Pan Assay Interference Compounds (PAINS) screening of the designed compounds was carried out via an online program “PAINS Remover” (<http://www.cbligand.org/PAINS/>), and all of the compounds passed the filter and were retained.

2.2. NOB and its derivatives reverse ABCB1-mediated MDR

The IC_{50} values of NOB and its derivatives against PTX-resistant HCT8/T cells (without adding 0.94 $\mu\text{mol/L}$ PTX to the culture medium) were listed in Table 1. These compounds showed anti-tumor effects against resistant human intestine and lung cancer cell lines, and their cytotoxicity are much lower than that of PTX (5.89 $\mu\text{mol/L}$ in HCT8/T).

The long-term colony formation assays further ascertained the enhanced anti-proliferative effect of NOB and its derivatives on A549/T and HCT8/T cells, as shown in Fig. 2A and B. We noticed that NOB, **13** and **29d** could inhibit MDR cancer cell colony formation in a dose-dependent manner. However, there is no difference in the inhibition of the colony formation among **13**, **29d** and NOB at their lowest effect dosage, indicating the similar reversal effects of NOB and its derivatives after long-time treatment.

As shown in Table 1, NOB and its derivatives enhanced the anti-tumor effects of PTX by decreasing its IC_{50} against the resistant HCT8/T cells. Specifically, the IC_{50} values of PTX in the presence of NOB, **7c**, **13** and **29d** were reduced by 185-, 81-, 66- and 87-fold, respectively. However, NOB, **7c**, **13** and **29d** did not affect the IC_{50} of PTX for the sensitive HCT8 cells (data not shown). In view of the relatively stronger cytotoxicity (38.46 $\mu\text{mol/L}$) of **7c** than that of NOB, only **13**, **29d** and NOB were selected for further studies.

2.3. Structure–activity relationships (SARs) of NOB and its derivatives

When a methoxy group was added at the C-5 position (**7c**) relative to **7b** (NOB), the affinity decreased since there was insufficient space for accommodation of another methoxy group. The presence of 1,3-benzodioxole (**7a**) was unfavorable to affinity due to steric hindrance. For inhibitors **23a** (one methoxy group), **23d** (two methoxy groups), **13** (two methoxy groups) and **7b** (three methoxy groups) with the same R_4 group, we found that more methoxy groups on the benzene ring A was propitious to better inhibitory potency, whereas the opposite phenomenon was observed on the R_4 position for **7b** (two methoxy groups) and **7c** (three methoxy groups). In addition, for inhibitors **13**, **16** and **18**, the bulky bromine atom of **16** or the NH_2 group of **18** at the R_1 group decreased the inhibitory affinity in comparison with the hydrogen atom of **13**^{16–18}.

On the basis of these results, we decided to retain the methoxy groups on the A and B rings and change the side chain at the X position. The dimethylaminoethyl sidechain of **29d** formed hydrophobic and van der Waals interactions with the residues of P-gp, which significantly differs from NOB. Therefore, other modifications such as replacement of methyl-ethyl-dimethylamine with 2-methoxyethyl (**29c**), H (**28**), Me (**29a**) or *n*-propyl (**29b**), were failed to improve their binding affinities. Thus, NOB, **29d** and **13** were selected for subsequent study.

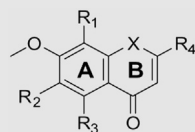
Moreover, the solubility data of NOB, **13** and **29d** were measured as 5.58 ± 1.17 , 3.67 ± 0.52 and 1.58 ± 0.13 mg/mL in sodium phosphate buffer (0.35 mol/L, pH = 7.3) at 25 °C, respectively, using the high-performance liquid chromatography (HPLC) approach. The presence of the dimethylaminoethyl sidechain of **29d** possibly accounts for the notable improvement in the water solubility of **29d** over NOB and **13** (280-fold higher), predicting that **29d** possibly has better performance *in vivo*.

2.4. Anti-tumor effects in A549/T xenograft model

We next evaluated whether synthesized NOB and its derivatives could overcome PTX resistance in the A549/T xenograft model. Based on previous study, PTX was administered *via* intraperitoneal (i.p.) route at an effective dose (15 mg/kg) for normal tumor¹⁹. As expected, PTX alone exhibited no effect on treating MDR tumors, as shown by similar tumor progression between the PTX treated group and vehicle control group, indicating resistance (Fig. 3). However, for the cocktail **29d** and PTX administration, **29d** at both 25 mg/kg and 50 mg/kg dosages significantly reduced the tumor volumes (Fig. 3B–D) compared with PTX alone, indicating considerable therapeutic efficacy. Moreover, there was no apparent weight loss observed in all nude mice (Fig. 3A), suggesting that the combination regimen did not bring additional toxicity. Notably, **29d** (50 mg/kg) with PTX greatly reduced the volumes of tumors by 57% in the A549/T xenograft model, which is more effective than NOB at the same dosage ($P < 0.05$). Similarly, NOB derivative **13** also enhanced the therapeutic efficacy of PTX in the A549/T xenograft model (Fig. 4). However, the tumor growth inhibition effect of **13** is similar to that of NOB.

2.5. Both **29d** and **13** potentiate apoptosis induced by PTX

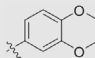
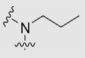
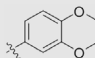
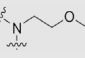
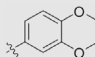
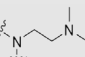
Consistent with the effects of NOB, **29d** and **13** significantly potentiated the apoptosis induced by PTX, as shown in Fig. 5A and B, while PTX (5.89 $\mu\text{mol/L}$), **29d** or **13** (9 $\mu\text{mol/L}$) alone did not induce cell apoptosis. Moreover, cell cycle progressions were evaluated by flow cytometry in asynchronously growing HCT8/T cells and sensitive HCT8 cells after treatment with PTX in the absence or presence of **29d** or **13**. When 0.94 $\mu\text{mol/L}$ PTX was added to the culture medium of HCT8/T for maintaining resistance, 71.9% of cells in G1 phase and 17.1% of cells in G2 phase after incubation were observed, which is similar to the phase ratios in the vehicle group, as shown in Fig. 5C and D. However, PTX (0.94 $\mu\text{mol/L}$) treated with **29d** or **13** (9 $\mu\text{mol/L}$) for 48 h resulted in significant G2M arrest (>80%) in HCT8/T cells. Therefore, **29d** or **13** significantly enhanced the cell growth inhibition, apoptosis and G2M cell cycle arrest induced by 0.94 $\mu\text{mol/L}$ PTX, although HCT8/T cells were remarkably resistant to 0.94 $\mu\text{mol/L}$ PTX.

Table 1 Nobiletin (NOB) and its derivatives reduce the IC₅₀ of paclitaxel (PTX) for multidrug resistant HCT8/T cancer cells.

Compd.	R ₁	R ₂	R ₃	R ₄	X	Cytotoxicity IC ₅₀ (μmol/L) ^a	Cytotoxicity of combination IC ₅₀ (μmol/L) ^b	Reversal fold ^c
PTX	—	—	—	—	—	5.89 ± 0.24	5.89 ± 0.24	1
7a	OMe	OMe	OMe		O	>100	0.14 ± 0.01	43
7b (NOB)	OMe	OMe	OMe		O	44.67 ± 3.83	0.030 ± 0.002	185
7c	OMe	OMe	OMe		O	38.46 ± 3.30	0.080 ± 0.004	81
13	H	OMe	OMe		O	74.99 ± 4.04	0.090 ± 0.005	66
16	Br	OMe	OMe		O	>100	0.15 ± 0.01	40
18	NH ₂	OMe	OMe		O	66.83 ± 3.99	0.29 ± 0.05	21
23a	OMe	H	H		O	66.83 ± 2.73	0.29 ± 0.01	21
23b	OMe	H	H		O	69.98 ± 6.78	0.44 ± 0.04	14
23c	OMe	H	H		O	39.36 ± 4.41	0.36 ± 0.02	17
23d	OMe	OMe	H		O	66.83 ± 2.73	0.13 ± 0.01	47
28	OMe	OMe	OMe		NH	>100	0.23 ± 0.02	27
29a	OMe	OMe	OMe		NMe	26.61 ± 2.63	0.11 ± 0.01	55

(continued on next page)

Table 1 (continued)

Compd.	R ₁	R ₂	R ₃	R ₄	X	Cytotoxicity IC ₅₀ (μmol/L) ^a	Cytotoxicity of combination IC ₅₀ (μmol/L) ^b	Reversal fold ^c
29b	OMe	OMe	OMe			21.13 ± 1.77	0.15 ± 0.01	40
29c	OMe	OMe	OMe			59.57 ± 3.62	0.24 ± 0.01	26
29d	OMe	OMe	OMe			>100	0.070 ± 0.008	87

–Not applicable.

^aIntrinsic cytotoxicity of target compounds or PTX alone to HCT8/T cells.

^bValues of IC₅₀ for cytotoxicity of combination (P-gp inhibitor 10 μmol/L + PTX) were as mean ± SD of at least three independent experiments.

^cThe reversal fold was calculated as a ratio of IC₅₀ (PTX) to IC₅₀ (P-gp inhibitor 10 μmol/L + PTX).

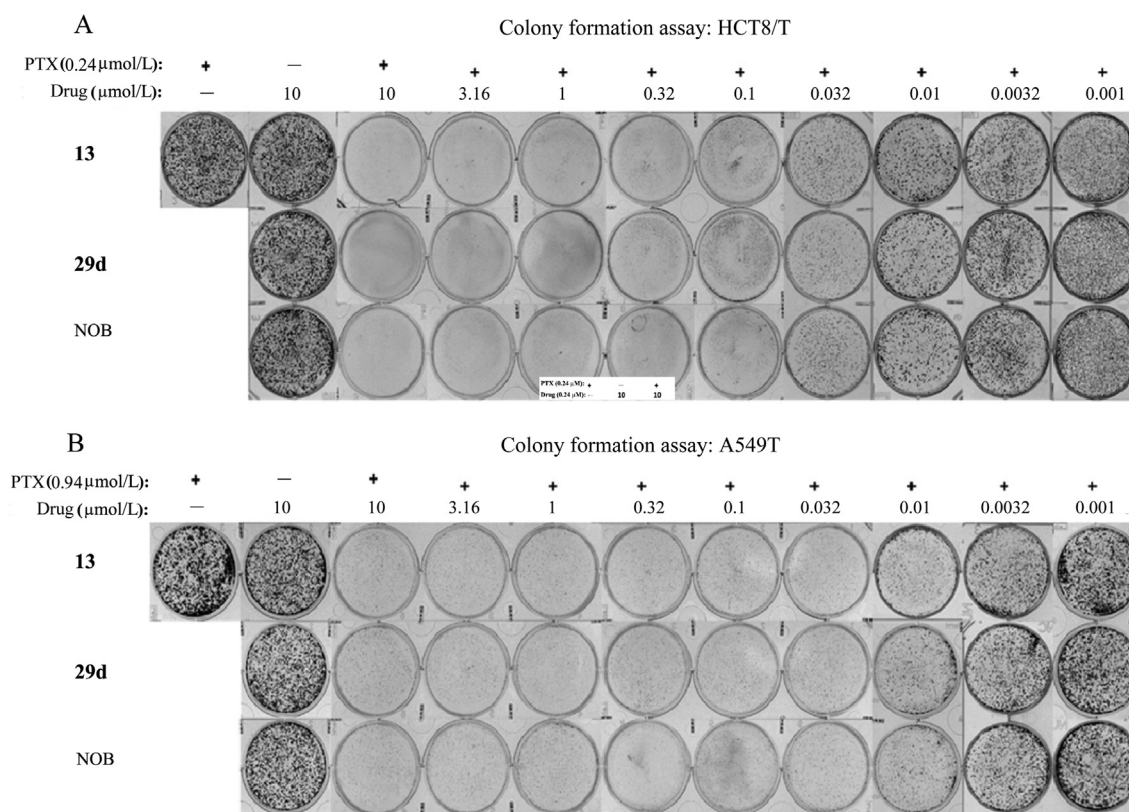


Figure 2 NOB and its derivatives reverse the resistance of paclitaxel (PTX) to P-gp-overexpressing MDR cancer cells. **29d**, **13** and NOB enhanced the anti-proliferative effects of PTX in two drug-resistant cancer cell lines, HCT8/T (A) and A549/T (B), in a dose-dependent manner according to the colony formation assay. The cells were treated with PTX (0.24 μmol/L for A549/T and 0.94 μmol/L for HCT8/T for maintaining the resistance of cancer cells) in the presence or absence of **29d**, **13** and NOB at the indicated concentrations.

2.6. **29d** and **13** inhibit the P-gp function

We also evaluated the modulating effects of synthesized NOB and its derivatives on P-gp by evaluating the accumulation of P-gp substrates, including doxorubicin (DOX) and flutax-2 (a fluorescent PTX derivative), using fluorescence microscopy and

flow cytometry analysis. Enhanced intracellular accumulations of DOX or flutax-2 by NOB and its derivatives were confirmed by flow cytometry analysis, as shown in Fig. 6A and C. Moreover, stronger fluorescence signals of DOX and flutax-2 were observed by adding NOB, **29d**, **13** and quinidine (QND, positive control), as shown in Fig. 6B and D. The effects of **29d** on the

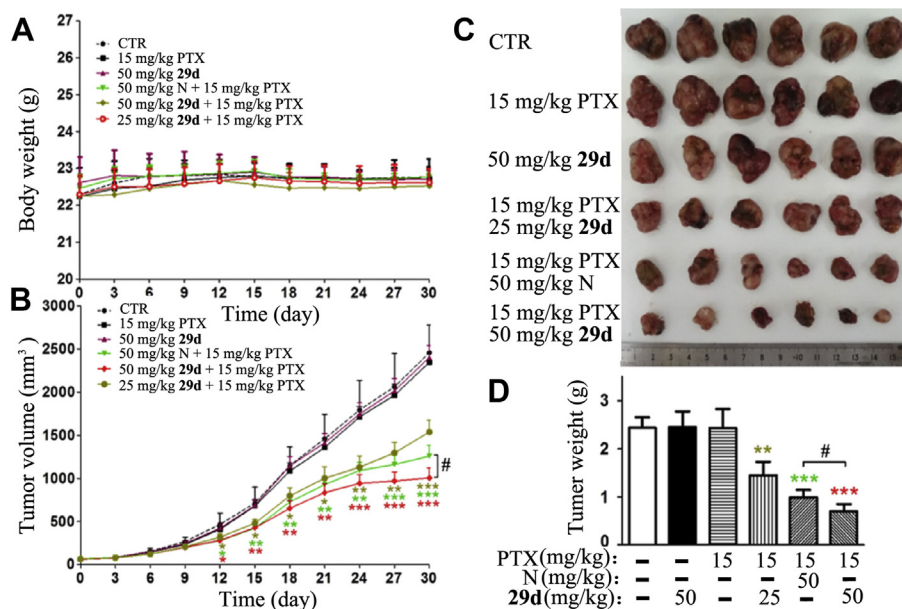


Figure 3 NOB (N) and its derivative **29d** enhanced the anticancer effect of PTX in the PTX-resistance A549/T cell nude mouse xenograft model. The changes in body weight (A) and tumor growth curves (B) were recorded after A549/T cell implantation. The excised tumors were photographed (C) and weighed (D) on day 30 after implantation. The data were shown as mean \pm SD for each group ($n = 6$), * $P < 0.05$, ** $P < 0.01$, *** $P < 0.001$ vs. PTX alone; # $P < 0.05$ vs. administered PTX and NOB. CTR, the control group.

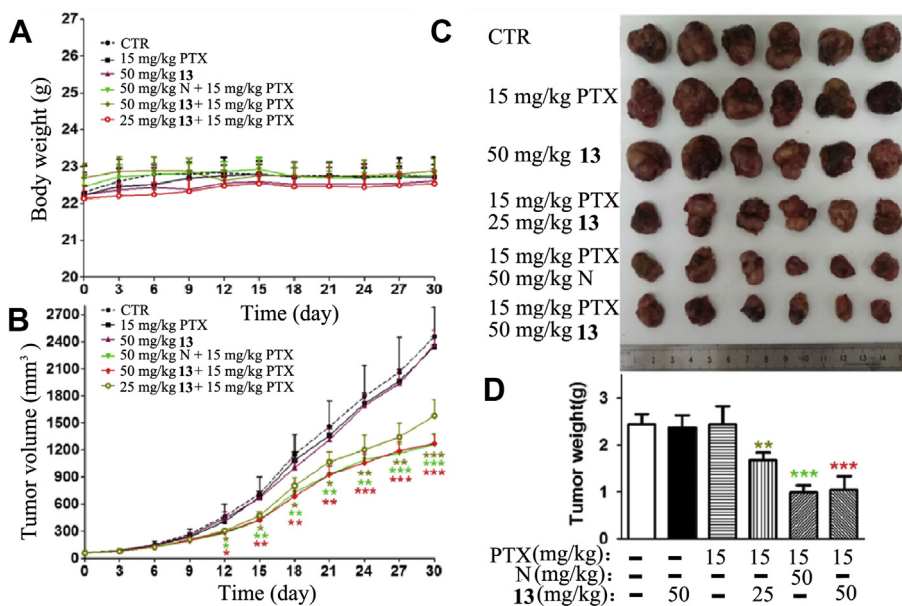


Figure 4 NOB (N) and its derivative **13** enhanced the anticancer effect of PTX in the PTX resistance A549/T cell nude mouse xenograft model. The changes in body weight (A) and tumor growth curves (B) were recorded after A549/T cell implantation. The excised tumors were photographed (C) and weighed (D) on day 30 after implantation. The data were shown as mean \pm SD for each group ($n = 6$), * $P < 0.05$, ** $P < 0.01$, *** $P < 0.001$ vs. PTX alone.

intracellular accumulation were stronger than those of **13** and NOB.

LC-MS/MS was used to detect the contents of PTX, **29d** and NOB in the tumors growing in the A549T xenograft model after treatment. Compared with the PTX alone group, NOB enhanced the content of PTX in tumors by 2.93-fold, while **29d** enhanced by 4.82-fold, which was approximately 1.65-fold that of NOB

(Fig. 7A). Moreover, the concentration of **29d** in tumor tissues was significantly increased by 1.72-fold in the PTX+**29d** (50 mg/kg) group compared with the **29d** (50 mg/kg) group (Fig. 7B), indicating that **29d** and PTX were competing for binding on P-gp. All of these results suggested that synthesized NOB and its derivatives could inhibit P-gp function in MDR cancer cells which led to increased intracellular chemotherapeutic agents to kill the MDR

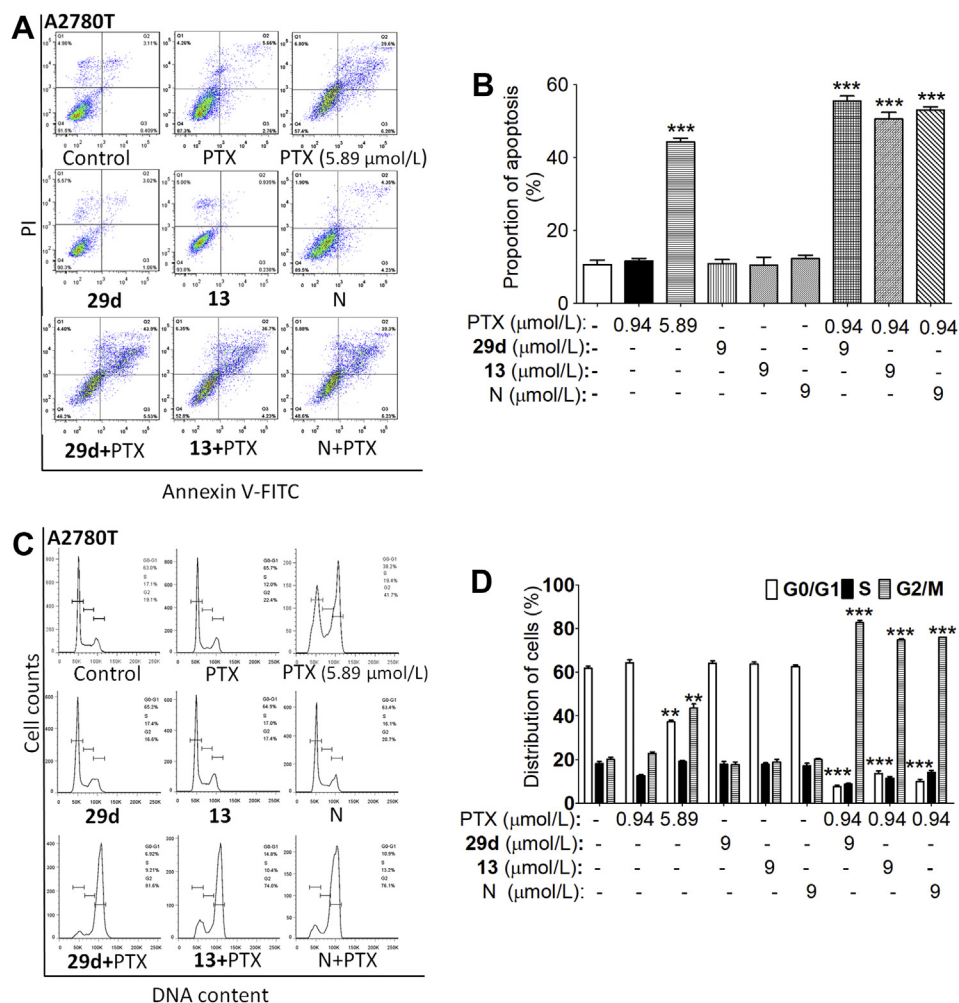


Figure 5 The effects of **29d**, **13** and NOB (N) on the apoptosis and cell cycle of HCT8/T induced by PTX. (A) **29d**, **13** and NOB at 9 μmol/L increased the proportion of apoptosis induced by 0.94 μmol/L PTX. (B) Addition of **29d**, **13** or NOB to medium containing 0.94 μmol/L PTX increased the percentage of cells in G2M phase, as exhibited by flow cytometry. The data were obtained from three different experiments and shown as mean ± SD ($n = 3$). $^{**}P < 0.01$, $^{***}P < 0.001$ vs. absence of **29d**, **13** or N.

cancer, and **29d** exhibited a stronger inhibition effect on the function of P-gp than **13** and NOB.

2.7. Putative binding pattern of **29d** to the pocket of P-gp

To show the putative binding pattern, **29d** was docked by the Surflex-dock module embedded in Tripos Sybyl X 2.0 (St. Louis, USA) to the crystal structure of P-gp in complex with QZ59-RRR (PDB ID: 4M2S). The selected binding pose of **29d** fitted the binding pocket well, with Surflex docking score (Total-Score) of 6.2274. In this binding modes (Fig. 8 and Supporting Information Section 1), several kinds of specific interactions between **29d** and P-gp were observed. Inhibitor **29d** formed two H-bonds with Tyr306 and Gln721, respectively. Strong π - π and π - σ interactions were also observed for **29d** with residues Phe979, Phe339, Phe724 and Phe728. In addition to van der Waals interactions and hydrophobic interactions with residues of Phe299, Gln986, Ile302 and Ser725, the dimethylaminoethyl sidechain of **29d** formed extra interactions with Leu335 and Phe331, which significantly differed from NOB¹⁰.

Subsequently, molecular dynamics (MD) simulations were applied for a more precise prediction of binding patterns using AMBER 14. As a result, the predicted binding free energies of the P-gp/**29d** and P-gp/NOB complexes were -43.99 ± 3.12 and -39.47 ± 2.62 kcal/mol, respectively. From the MD simulation results, apparent hydrophobic interactions with residues Phe299, Phe724, Phe728, Phe979 and Leu336 in P-gp were observed by **29d** and NOB. In addition, **29d** and NOB formed hydrogen bonds with Gln721 and Tyr306, respectively. Nevertheless, dimethylaminoethyl chain of **29d** formed extra van der Waal interactions with Phe339 and Ile302, which might account for its more negative binding free energy compared with NOB.

2.8. NOB and its derivatives overcome MDR via AKT/ERK/NRF2 pathway

Multiple targets are characteristics of natural products and ultimately offer clinical benefits in comparison with the three generations of MDR inhibitors²⁰. To explore the underlying

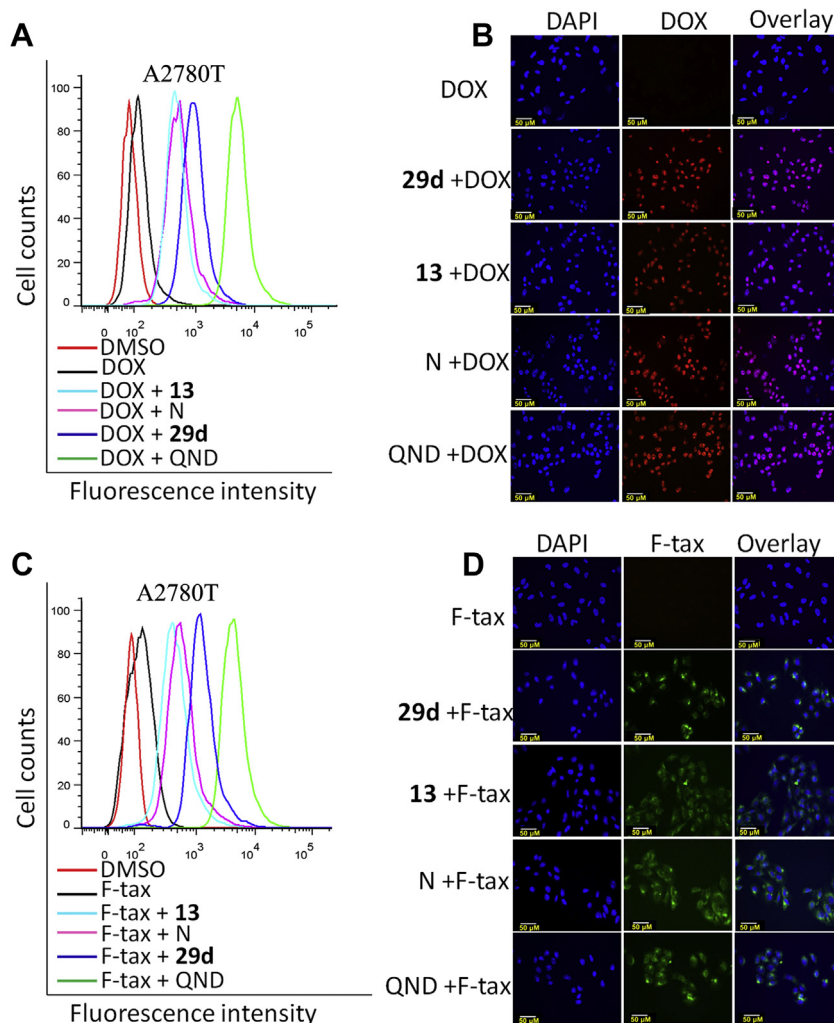


Figure 6 Effects of **29d**, **13** and NOB (N) on intracellular accumulation of DOX and Flutax-2 in HCT8T cells. HCT8/T cells were treated with 5 $\mu\text{mol/L}$ DOX (A) and (B) or 1 $\mu\text{mol/L}$ Flutax-2 (C) and (D) for 6 h in the absence or presence of 9 $\mu\text{mol/L}$ **29d**, **13**, NOB and 20 $\mu\text{mol/L}$ QND as indicated. Intracellular DOX or Flutax-2 were observed with a fluorescence microscope (B) and (D) and evaluated by measuring fluorescence with flow cytometry (A) and (C). The experiments were repeated 3 times, and representative images were presented.

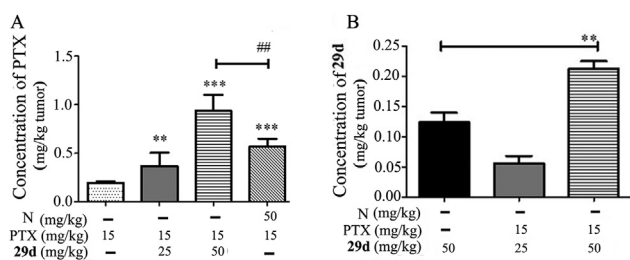


Figure 7 The concentrations of PTX (A) and **29d** (B) in MDR tumors after treatment with PTX alone or the combination of **29d** and NOB (N). The concentrations of PTX or **29d** in the tumor were evaluated with HPLC-MS, as described in contents. The data were shown as mean \pm SD for each group ($n = 6$), ** $P < 0.01$, *** $P < 0.001$ vs. PTX alone or **29d** alone; ## $P < 0.01$ vs. PTX + NOB.

mechanisms for functions of NOB and its derivatives, we evaluated the signaling pathways (Fig. 9) of NRF2/PI3K/AKT and ERK, which had been shown to be closely associated with resistance to chemotherapy drugs¹⁶. Interestingly, we found that *Nrf2*, phosphorylated AKT and ERK were significantly reduced in HCT8/T cells after administration of NOB, **29d** or **13**, while the expression of total AKT and ERK remained the same (Fig. 9). These results indicated that the MDR reversal effects of **29d** and **13** to chemotherapy agents were produced by the inhibition of *Nrf2*/PI3K/AKT pathways, the same as NOB.

Change of sensitivity of the MDR cancer cells to drugs could be due to reduction of ABCB1 expression, competitive inhibition of the ABCB1 transporter, or both. Therefore, we evaluated the effects of synthesized NOB, **29d** and **13** on the expression of

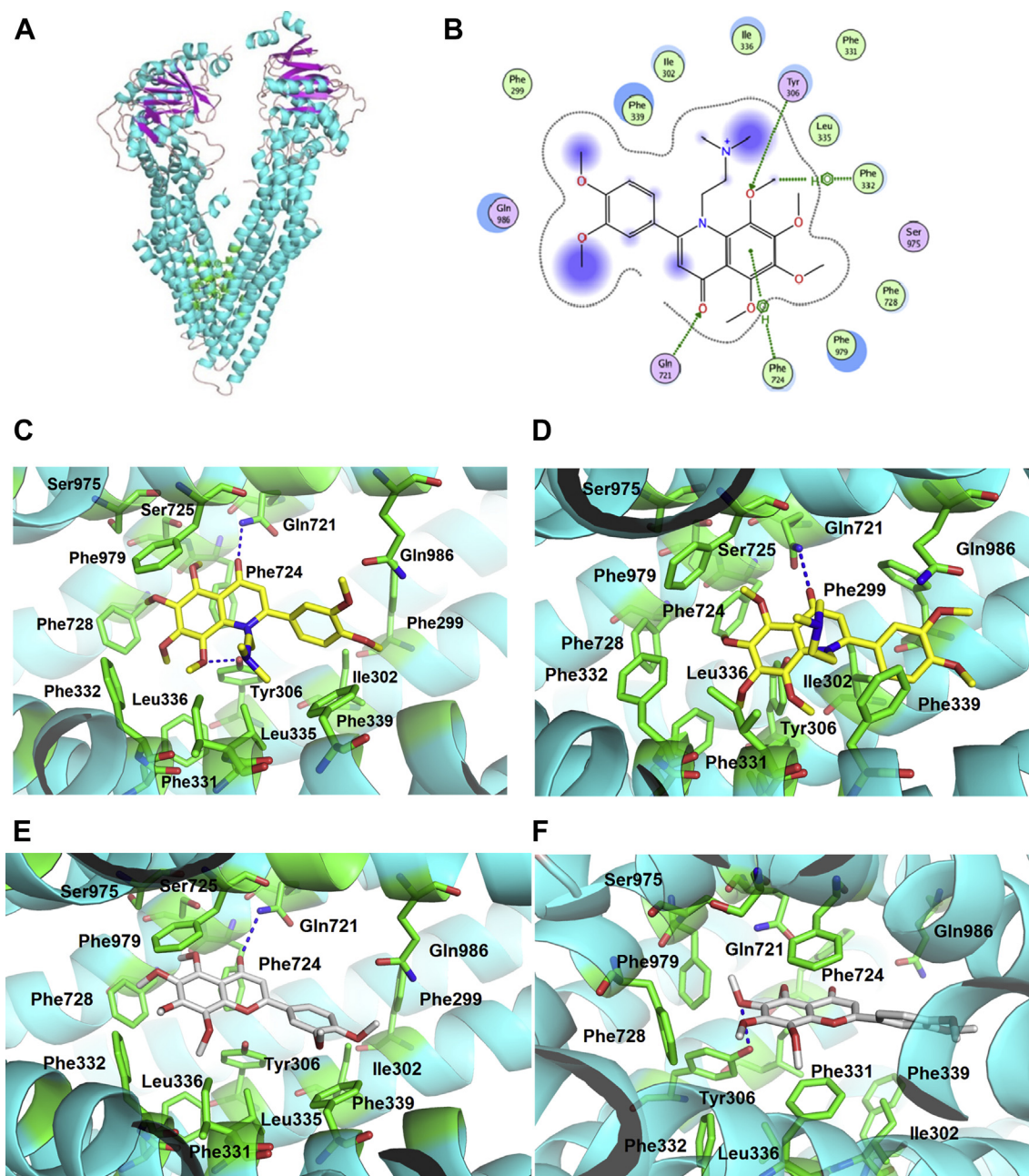


Figure 8 Binding patterns of **29d** (A–D, yellow in C and D) and NOB (E and F, grey) with P-gp (cyan) by docking and MD simulation methods. (A) Ribbon diagram of P-gp with docked **29d** (green). (B) Two-dimensional interaction mode between docked **29d** and P-gp. The interactions between **29d** and P-gp (green sticks). Hydrogen bonds are depicted by dashed blue. Hydrogen bonds and π - π/σ - π interactions are shown by green lines. Green and purple bubbles represent hydrophobic and polar amino acid residues, respectively. (C) and (E) refer to the binding patterns by docking method while (D) and (F) refer to the binding patterns by MD method. Therein, hydrogen bonds are depicted by dashed blue lines.

ABCB1. Interestingly, none of them at the reversal concentrations alter the protein level of ABCB1 in HCT8/T cells (Fig. 9). In addition, NOB and its derivatives did not affect the expression of BCRP and MDR1 in A549/T cells (Fig. 10) which are two major efflux transporters related to the PTX resistance. Thus, synthesized NOB and its derivatives likely inhibited ABCB1 transporter function but did not affect the expression of ABCB1.

Several metabolites of NOB including 3'-demethylnobiletin, 4'-demethylnobiletin, 3',4'-didemethylnobiletin (DTF), 5-

demethylnobiletin, 5,3'-didemethylnobiletin, 5,4'-didemethylnobiletin and 5,3',4'-tridemethylnobiletin have been identified as the major metabolites from the urine of mouse by the optimized HPLC method^{21–22}. Anti-inflammatory effects of 4'-demethylnobiletin on TPA-induced mice ear inflammation have been shown through inhibition of PI3K/AKT/ERK phosphorylation²². Therefore, the metabolites of NOB derivatives possibly have inhibitory activity on P-gp function *via* the NRF2/PI3K/AKT pathways.

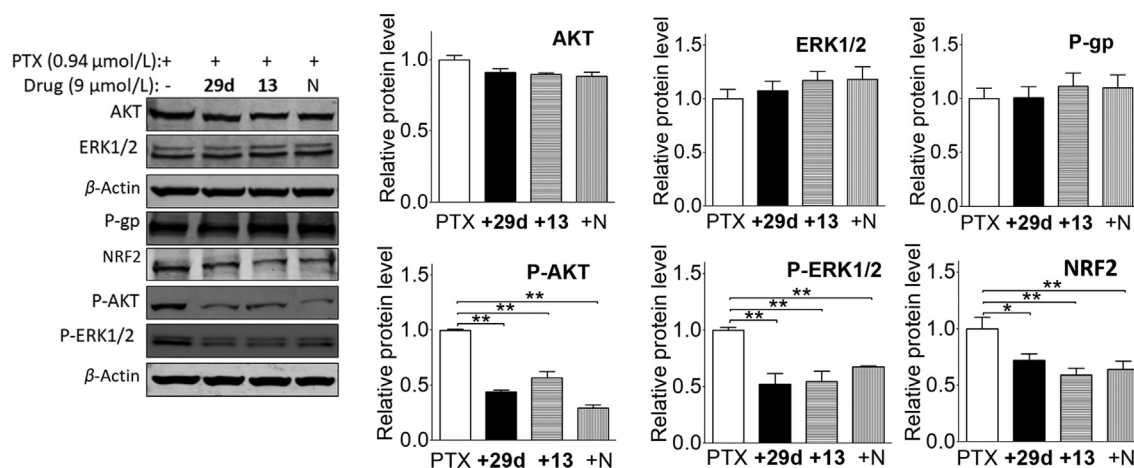


Figure 9 Effects of the combination treatment of PTX with **29d**, **13** and NOB (N) on expressions of P-gp, AKT, ERK and NRF2 in HCT8/T cells. Cells were treated with 9 $\mu\text{mol/L}$ **29d**, **13** and N for 48 h. Equal amounts of total lysate were used for Western blot. Combination treatment of PTX with **29d**, **13** or NOB did not influence P-gp expression, but reduced the level of NRF2 as well as the phosphorylation of AKT/ERK. The experiments were repeated three times. The data were shown as mean \pm SD. * $P < 0.05$ and ** $P < 0.01$.

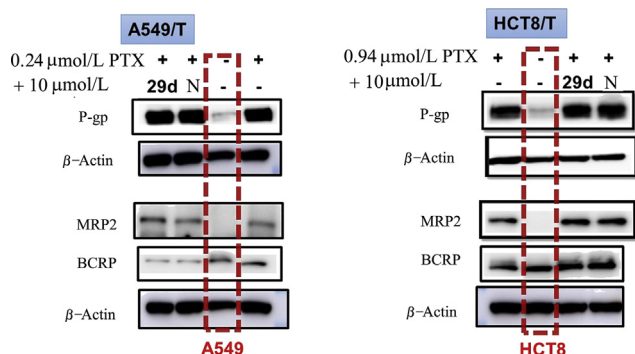


Figure 10 The expression of efflux transporters P-gp, MRP2 and BCRP in A549/T and HCT8/T cells, and the effects of **29d** and NOB (N) on their expression by comparing with sensitive A549 or HCT8 cells (red frame). Cells were treated with 9 $\mu\text{mol/L}$ **29d** or N for 48 h. Equal amounts of total lysate were loaded and detected by Western blot.

3. Conclusions

In short, NOB was produced with a high yield by total synthesis of six steps and fourteen derivatives were synthesized to discover potent compounds with remarkable solubility and efficacy as MDR reversal agents. Among them, **29d** showed 280-fold higher water solubility than NOB and **13**. As a result, **29d** significantly increased PTX concentration in the tumor *in vivo* and showed a stronger tumor growth inhibition than NOB and **13** after co-administered with PTX. Moreover, our studies demonstrated that the activated NRF2/PI3K/AKT pathways in MDR cancer cells were remarkably inhibited by the conjunction of **29d** and PTX.

4. Experimental

4.1. Chemicals and reagents

PTX, DOX, verapamil (Ver), QND, rhodamine 123 (Rho123), dimethyl sulfoxide (DMSO), propidium iodide (PI), trichloroacetic acid (TCA), crystal violet, sulforhodamine B (SRB) and

other chemicals were purchased from Sigma–Aldrich (St. Louis, USA). The flutax-2, RPMI 1640 medium, fetal bovine serum, penicillin and streptomycin were obtained from Life Technologies, Inc. (Grand Island, USA). P-gp antibodies were purchased from Calbiochem (cat. No. 517310). ERK1/2 and actin antibodies were purchased from Santa Cruz Biotechnology, USA. AKT, P-AKT and P-ERK1/2 were purchased from Cell Signaling Technology, Inc. (Boston, USA).

All starting materials and reagents were purchased from commercial suppliers (Sigma–Aldrich, Adamas, Energy, Bide, ShuYa, J&K and Meryer, Shanghai, China) and used directly without further purification. Chemical HG/T2354-92 silica gel (200–300 mesh, Haiyang[®], Qingdao, China) was used for chromatography, and silica gel plates with fluorescence F254 (0.25 mm, Huanghai[®], Qingdao, China) were used for thin-layer chromatography (TLC) analysis. Reactions requiring anhydrous conditions were performed under argon or with a calcium chloride tube. ¹H NMR and ¹³C NMR spectra were recorded at room temperature (rt) on a Bruker AVANCE III 400 instrument (Germany) with tetramethylsilane (TMS) as an internal standard. The following abbreviations are used: s (singlet), br s (broad singlet), d (doublet), dd (doublet of doublets), t (triplet), q (quartet) and m (multiplet). Coupling constants were reported in Hz. High-resolution mass spectra (HRMS) were recorded on SHIMADZU LCMS-IT-TOF (Kyoto, Japan). The purities of compounds were determined by reverse-phase HPLC analysis, confirming purity to exceed 95%. HPLC instrument: SHIMADZU LC-20AT (column: Hypersil BDS C18, 5.0 μm , 150 mm \times 4.6 mm (Elite); detector: SPD-20A UV/VIS detector, UV detection at 254 nm; elution, MeOH in water (80%, v/v); T = 25 $^{\circ}\text{C}$; flow rate = 1.0 mL/min; Kyoto, Japan).

4.1.1. 3,4,5-Trimethoxyphenyl acetate (**2**)

A mixture of **1** (9.2 g, 50 mmol) and sodium acetate (8.2 g, 100 mmol) in acetic anhydride (47 mL, 500 mmol) was heated at 110 $^{\circ}\text{C}$ for 2 h. TLC analysis (petroleum ethe/ethyl acetate = 7:3) showed completion of the reaction. Then the reaction mixture was concentrated under reduced pressure, diluted with water and extracted with ethyl acetate thrice. The organic phase was washed

with brine, dried over anhydrous sodium sulfate. The organic layer was concentrated to afford the product **2** (11.2 g) as a white solid, which was used directly in the next step without further purification. Yield: 91%. $^1\text{H NMR}$ (CDCl_3 , 400 MHz) δ 6.34 (s, 2H), 3.83 (s, 9H), 2.29 (s, 3H).

4.1.2. 1-(6-Hydroxy-2, 3, 4-trimethoxyphenyl) ethanone (**3**)

Boron trifluoride etherate (ca. 48% BF_3 , 250 mL) was added to a solution of **2** (11.2 g, 50 mmol) in glacial acetic acid (37.5 mL). The reaction mixture was stirred at 70 °C for 2 h. TLC analysis (petroleum ether/ethyl acetate = 7:3) showed completion of reaction. Then the reaction mixture was quenched with water and extracted with ethyl acetate. The organic phase was washed with brine, dried over anhydrous sodium sulfate, and purified by silica gel column chromatography (petroleum ether/ethyl acetate = 10:1) to afford product **3** (10.2 g) as a yellow oil. Yield: 91%. $^1\text{H NMR}$ (CDCl_3 , 500 MHz): δ 13.44 (s, 1H), 6.24 (s, 1H), 3.99 (s, 3H), 3.89 (s, 3H), 3.78 (s, 3H), 2.66 (s, 3H).

4.1.3. 1-(2-Hydroxy-3-iodo-4,5,6-trimethoxyphenyl) ethanone (**4**)

Adding NIS (1.4 g, 6.0 mmol) and *p*-toluenesulfonic acid monohydrate (950 mg, 5.0 mmol) to a stirred solution of **3** (1.1 g, 5.0 mmol) in CH_3CN (50 mL). The mixture was stirred at rt for 2 h until the start material disappeared as monitored by TLC. After evaporated under vacuum, the reaction mixture was extracted with ethyl acetate. The organic phase was washed with saturated aqueous sodium thiosulfate and brine, and dried over anhydrous sodium sulfate. The solvent was evaporated to afford product **4** as a yellow-green solid, which was used directly in the next step without further purification. Yield: 73%. $^1\text{H NMR}$ (500 MHz, CDCl_3) δ 14.00 (s, 1H), 4.02 (d, $J = 4.6$ Hz, 3H), 4.01 (s, 3H), 3.80 (s, 3H), 2.70 (s, 3H).

4.1.4. 1-(2-Hydroxy-3,4,5,6-tetramethoxyphenyl) ethanone (**5**)

Copper chloride (359 mg, 3.6 mmol) was added to a solution of **4** (3.6 g, 10.2 mmol) in DMF (30 mL) under an atmosphere of Ar at rt. Then freshly prepared 4.0 mol/L solution of sodium methoxide in methanol (25 mL, 102 mmol) was added to the mixture at 90 °C for 20 min. After cooling, the solution was poured into ice and acidified with 5.0 mol/L HCl. The organic layer was extracted with ethyl acetate. The combined organic extracts were washed with brine and dried over anhydrous sodium sulfate, and purified by silica gel column chromatography (petroleum ether/ethyl acetate = 10:1) to afford product **5** (1.5 g) as a light yellow-green liquid. Yield: 59%. $^1\text{H NMR}$ (500 MHz, CDCl_3) δ 13.16 (s, 1H), 4.08 (s, 3H), 3.94 (s, 3H), 3.86 (s, 3H), 3.81 (s, 3H), 2.68 (s, 3H).

4.1.5. General procedure for synthesis of compounds **6a–6c**

To a solution of **5** (128 mg, 0.5 mmol) in dichloromethane (2.5 mL) was added triethylamine (208 μL , 1.5 mmol) and acyl chlorides (0.65 mmol) at 0 °C. The mixture was stirred at rt for 2 h. Then the reaction mixture was quenched with water and extracted with ethyl acetate. The organic phase was washed with brine, dried over anhydrous sodium sulfate, and purified by silica gel column chromatography (petroleum ether/ethyl acetate = 5:1) to afford the product as white solids.

4.1.5.1. 2-Acetyl-3,4,5,6-tetramethoxyphenyl benzo[d][1,3]dioxole-5-carboxylate (**6a**). White solid. Yield: 85%. $^1\text{H NMR}$ (400 MHz, CDCl_3) δ 7.78 (d, $J = 8.7$ Hz, 1H), 7.56 (s, 1H), 6.91

(d, $J = 4.8$ Hz, 1H), 6.07 (s, 2H), 3.98 (s, 3H), 3.93 (s, 3H), 3.90 (s, 3H), 3.81 (s, 3H), 2.47 (s, 3H).

4.1.5.2. 2-Acetyl-3,4,5,6-tetramethoxyphenyl 3,4-dimethoxybenzoate (**6b**). White solid. Yield: 80%. $^1\text{H NMR}$ (400 MHz, CDCl_3) δ 7.82 (dd, $J = 8.4$, 2.0 Hz, 1H), 7.63 (d, $J = 2.0$ Hz, 1H), 6.94 (d, $J = 8.5$ Hz, 1H), 3.98 (s, 3H), 3.97 (s, 3H), 3.95 (s, 3H), 3.94 (s, 3H), 3.90 (s, 3H), 3.81 (s, 3H), 2.47 (s, 3H).

4.1.5.3. 2-Acetyl-3,4,5,6-tetramethoxyphenyl 3,4,5-trimethoxybenzoate (**6c**). White solid. Yield: 90%. $^1\text{H NMR}$ (400 MHz, CDCl_3) δ 7.41 (s, 1H), 7.39 (s, 1H), 3.99 (s, 4H), 3.96 (s, 3H), 3.95 (s, 3H), 3.94 (s, 3H), 3.93 (s, 6H), 3.90 (s, 3H), 3.83 (s, 3H), 2.49 (s, 3H).

4.1.6. General procedure for synthesis of compounds **7a–7c**

To a solution of **6** (0.4 mmol) in dichloroethane (2.4 mL) was added triethylamine (166 μL , 1.2 mmol) and trimethylsilyl trifluoromethanesulfonate (434 μL , 2.4 mmol). The mixture was stirred at 95 °C for 2 h, then quenched with CH_3OH , and extracted with ethyl acetate. The organic phase was washed with brine, dried over anhydrous sodium sulfate, and purified by silica gel column chromatography (petroleum ether/ethyl acetate = 2:1) to afford the product.

4.1.6.1. 2-(Benzo[d][1,3]dioxol-5-yl)-5,6,7,8-tetramethoxy-4H-chromen-4-one (**7a**). White solid. Yield: 75%. Purity: 99%. $^1\text{H NMR}$ (400 MHz, $\text{MeOD-}d_4$) δ 7.62 (dd, $J = 8.3$, 1.6 Hz, 1H), 7.47 (d, $J = 1.6$ Hz, 1H), 7.02 (d, $J = 8.3$ Hz, 1H), 6.66 (s, 1H), 6.11 (s, 2H), 4.12 (s, 3H), 4.03 (s, 3H), 3.94 (s, 3H), 3.90 (s, 3H). $^{13}\text{C NMR}$ (126 MHz, CDCl_3) δ 177.33, 160.86, 151.46, 150.51, 148.50, 148.38, 147.67, 144.13, 138.07, 125.54, 121.15, 114.86, 108.85, 107.12, 106.12, 101.90, 62.28, 62.07, 61.8, 61.68. HR-MS (ESI) m/z Calcd. $\text{C}_{20}\text{H}_{19}\text{O}_8^+$ [$\text{M}+\text{H}$] $^+$ 387.1074, Found 387.1073.

4.1.6.2. 2-(3,4-Dimethoxyphenyl)-5,6,7,8-tetramethoxy-4H-chromenone (**7b**). White solid. Yield: 78%. Purity: 99%. $^1\text{H NMR}$ (500 MHz, CDCl_3) δ 7.57 (d, $J = 8.2$ Hz, 1H), 7.42 (s, 1H), 7.00 (d, $J = 8.3$ Hz, 1H), 6.62 (s, 1H), 4.11 (s, 3H), 4.03 (s, 3H), 3.98 (s, 3H), 3.97 (s, 3H), 3.96 (s, 6H). $^{13}\text{C NMR}$ (126 MHz, CDCl_3) δ 177.35, 161.04, 151.92, 151.43, 149.28, 148.42, 147.72, 144.08, 138.01, 124.00, 119.62, 114.85, 111.22, 108.53, 106.88, 62.27, 61.98, 61.84, 61.69, 56.09, 55.97. HR-MS (ESI) m/z Calcd. $\text{C}_{21}\text{H}_{23}\text{O}_8^+$ [$\text{M}+\text{H}$] $^+$ 403.1389, Found 403.1389.

4.1.6.3. 5,6,7,8-Tetramethoxy-2-(3,4,5-trimethoxyphenyl)-4H-chromen-4-one (**7c**). White solid. Yield: 80%. Purity: 96%. $^1\text{H NMR}$ (400 MHz, CDCl_3) δ 7.17 (s, 2H), 6.64 (s, 1H), 4.11 (s, 3H), 4.03 (s, 3H), 3.96 (s, 12H), 3.93 (s, 3H). $^{13}\text{C NMR}$ (101 MHz, CDCl_3) δ 177.31, 160.80, 153.59, 151.55, 148.44, 147.70, 144.16, 141.07, 137.98, 126.69, 114.82, 107.63, 103.67, 103.39 \times 2, 62.26, 61.89, 61.81, 61.67, 61.03, 56.24 \times 2. HR-MS (ESI) m/z Calcd. $\text{C}_{22}\text{H}_{25}\text{O}_9^+$ [$\text{M}+\text{H}$] $^+$ 433.1493, Found 433.1483.

4.1.7. 2-Acetyl-3,4,5-trimethoxyphenyl 3,4-dimethoxybenzoate (**10**)

To a solution of **3** (904 mg, 4.0 mmol) in dichloromethane (16 mL) was added triethylamine (1.47 mL, 12 mmol) and 3,4-

dimethoxybenzoyl chloride (1.04 g, 5.2 mmol) at 0 °C. The mixture was stirred at rt for 2 h, then quenched with water, and extracted with ethyl acetate. The organic phase was washed with brine, dried over anhydrous sodium sulfate, and purified by silica gel column chromatography (petroleum ether/ethyl acetate = 5:1) to afford product **10** as a white solid. Yield: 85%. ¹H NMR (400 MHz, CDCl₃) δ 7.81 (dd, *J* = 8.4, 2.0 Hz, 1H), 7.63 (d, *J* = 2.0 Hz, 1H), 6.96 (d, *J* = 8.5 Hz, 1H), 6.59 (s, 1H), 3.98 (s, 3H), 3.97 (s, 6H), 3.91 (s, 3H), 3.90 (s, 3H), 2.51 (s, 3H).

4.1.8. 1-(3-Bromo-2-hydroxy-4,5,6-trimethoxyphenyl) ethanone (**11**)

Sodium acetate (1.77 g, 21.6 mmol) was added to a solution of **3** (4.436 g, 19.6 mmol) in glacial acetic acid (15 mL). Then Br₂ in glacial acetic acid (1.5 mL, 29.4 mmol) was added dropwise to the reaction mixture at 0 °C. The mixture was stirred at rt for 12 h and poured into ice water (150 mL). The solid was filtered and washed with water to yield product **11** as a yellow solid, which was used directly in the next step without further purification. Yield: 81%. ¹H NMR (400 MHz, CDCl₃) δ 13.75 (s, 1H), 4.05 (s, 3H), 4.04 (s, 3H), 3.83 (s, 3H), 2.72 (s, 3H).

4.1.9. 1-(2-Hydroxy-4,5,6-trimethoxy-3-nitrophenyl) ethanone (**12**)

Nitric acid (ca. 70% HNO₃, 621 μL, 14 mmol) was added dropwise to **3** (1.58 g, 7 mmol) over 15 min at 0 °C. Then the reaction mixture was quenched with water and extracted with ethyl acetate. The organic phase was washed with brine, dried over anhydrous sodium sulfate, and purified by silica gel column chromatography (petroleum ether/ethyl acetate = 5:1) to afford product **12** as a yellow solid. Yield: 79%. ¹H NMR (400 MHz, CDCl₃) δ 13.56 (s, 1H), 4.10 (s, 3H), 4.07 (s, 3H), 3.81 (s, 3H), 2.69 (s, 3H).

4.1.10. 2-(3,4-Dimethoxyphenyl)-5,6,7-trimethoxy-4H-chromen-4-one (**13**)

To a solution of **10** (1.17 g, 3.0 mmol) in dichloroethane (18 mL) was added triethylamine (1.2 mL, 9.0 mmol) and trimethylsilyl trifluoromethanesulfonate (3.3 mL, 18 mmol). The mixture was then stirred at 95 °C for 2 h, quenched with CH₃OH, and extracted with ethyl acetate. The organic phase was washed with brine, dried over anhydrous sodium sulfate, and purified by silica gel column chromatography (petroleum ether/ethyl acetate = 2:1) to afford product **13** (905 mg) as a brown solid. Yield: 81%. Purity: 99%. ¹H NMR (500 MHz, CDCl₃) δ 7.51 (d, *J* = 8.4 Hz, 1H), 7.33 (s, 1H), 6.98 (d, *J* = 8.4 Hz, 1H), 6.81 (s, 1H), 6.60 (s, 1H), 4.00 (s, 6H), 3.99 (s, 3H), 3.97 (s, 3H), 3.93 (s, 3H). ¹³C NMR (126 MHz, CDCl₃) δ 177.28, 161.17, 157.68, 154.51, 152.57, 151.79, 149.25, 140.35, 124.08, 119.59, 112.85, 111.10, 108.60, 107.37, 96.26, 62.21, 61.57, 56.33, 56.12, 56.08. HR-MS (ESI) *m/z* Calcd. C₂₀H₂₁O₇⁺ [M+H]⁺ 373.1282, Found 373.1285.

4.1.11. 2-Acetyl-6-bromo-3,4,5-trimethoxyphenyl 3,4-dimethoxybenzoate (**14**)

To a solution of **11** (1.2 g, 4.0 mmol) in dichloromethane (20 mL) was added triethylamine (1.4 mL, 12 mmol) and 3,4-dimethoxybenzoyl chloride (1.0 g, 5.2 mmol) at 0 °C. The mixture was stirred at rt for 2 h, quenched with water and extracted with ethyl acetate. The organic phase was washed with brine, dried over anhydrous sodium sulfate, and purified by silica gel column chromatography (petroleum ether/ethyl acetate = 5:1)

to afford product **14** as a yellow solid. Yield: 75%. ¹H NMR (400 MHz, CDCl₃) δ 7.85 (dd, *J* = 8.4, 2.0 Hz, 1H), 7.64 (d, *J* = 2.0 Hz, 1H), 6.95 (d, *J* = 8.5 Hz, 1H), 3.97 (s, 3H), 3.96 (s, 3H), 3.95 (s, 3H), 3.95 (s, 3H), 3.94 (s, 3H), 2.49 (s, 3H).

4.1.12. 2-Acetyl-3,4,5-trimethoxy-6-nitrophenyl 3,4-dimethoxybenzoate (**15**)

To a solution of **12** (1.2 g, 5.0 mmol) in dichloromethane (25 mL) was added triethylamine (1.8 mL, 15 mmol) and 3,4-dimethoxybenzoyl chloride (1.2 g, 6.0 mmol) at 0 °C. The mixture was stirred at rt for 2 h, quenched with water and extracted with ethyl acetate. The organic phase was washed with brine, dried over anhydrous sodium sulfate, and purified by silica gel column chromatography (petroleum ether/ethyl acetate = 5:1) to afford product **15** as a beige solid. Yield: 90%. ¹H NMR (500 MHz, CDCl₃) δ 7.73 (dd, *J* = 8.5, 2.0 Hz, 1H), 7.52 (d, *J* = 2.0 Hz, 1H), 6.92 (d, *J* = 8.5 Hz, 1H), 4.06 (s, 3H), 4.02 (s, 3H), 3.96 (s, 3H), 3.95 (s, 3H), 3.93 (s, 3H), 2.52 (s, 3H).

4.1.13. 8-Bromo-2-(3,4-dimethoxyphenyl)-5,6,7-trimethoxy-4H-chromen-4-one (**16**)

To a solution of **14** (1.2 g, 2.6 mmol) in dichloroethane (15 mL) was added triethylamine (1.0 mL, 7.5 mmol) and trimethylsilyl trifluoromethanesulfonate (2.7 mL, 15 mmol). The mixture was stirred at 95 °C for 2 h, then quenched with CH₃OH and extracted with ethyl acetate. The organic phase was washed with brine, dried over anhydrous sodium sulfate, and purified by silica gel column chromatography (petroleum ether/ethyl acetate = 1:1) to afford product **16** (900 mg) as a white solid. Yield: 79%. Purity: 99%. ¹H NMR (400 MHz, CDCl₃) δ 7.64 (dd, *J* = 8.5, 2.1 Hz, 1H), 7.53 (d, *J* = 2.1 Hz, 1H), 7.00 (d, *J* = 8.5 Hz, 1H), 6.75 (s, 1H), 4.09 (s, 3H), 4.00 (s, 3H), 3.99 (s, 3H), 3.97 (s, 3H), 3.96 (s, 3H). ¹³C NMR (126 MHz, CDCl₃) δ 177.00, 161.45, 155.77, 152.70, 152.07, 150.43, 149.28, 144.61, 123.50, 119.94, 115.81, 111.21, 108.78, 106.53, 101.43, 62.34, 61.84, 61.58, 56.10, 56.00. HR-MS (ESI) *m/z* Calcd. C₂₀H₂₀O₇Br⁺ [M+H]⁺ 451.0387, Found 451.0392.

4.1.14. 2-(3,4-Dimethoxyphenyl)-5,6,7-trimethoxy-8-nitro-4H-chromen-4-one (**17**)

To a solution of **15** (1.9 g, 4.3 mmol) in dichloroethane (26 mL) was added triethylamine (1.7 mL, 13 mmol) and trimethylsilyl trifluoromethanesulfonate (4.6 mL, 256 mmol). The mixture was stirred at 95 °C for 2 h, then quenched with CH₃OH and extracted with ethyl acetate. The organic phase was washed with brine, dried over anhydrous sodium sulfate, and purified by silica gel column chromatography (petroleum ether/ethyl acetate = 1:1) to afford product **17** (1.5 g) as a brown solid. Yield: 84%. ¹H NMR (400 MHz, CDCl₃) δ 7.42 (dd, *J* = 8.5, 2.1 Hz, 1H), 7.28 (d, *J* = 2.1 Hz, 1H), 6.96 (d, *J* = 8.6 Hz, 1H), 6.63 (s, 1H), 4.17 (s, 3H), 4.05 (s, 3H), 3.97 (s, 3H), 3.96 (s, 3H), 3.96 (s, 3H).

4.1.15. 8-Amino-2-(3,4-dimethoxyphenyl)-5,6,7-trimethoxy-4H-chromen-4-one (**18**)

To a solution of **17** (140 mg, 0.33 mmol) in tetrahydrofuran (25 mL) was added Pd/C catalyst (21 mg, 15%) under an atmosphere of H₂ at 40 °C for 15 h. After cooling to rt, the mixture was filtered with diatomite and washed with ethyl acetate. The organic layer was evaporated under vacuum to afford a residue, which was purified by silica gel column chromatography (petroleum ether/

ethyl acetate = 2:1) to yield product **18** (121 mg) as a yellow solid. Yield: 95%. Purity: 99%. ^1H NMR (400 MHz, CDCl_3) δ 7.50 (dd, J = 8.4, 2.0 Hz, 1H), 7.30 (d, J = 2.0 Hz, 1H), 6.98 (d, J = 8.5 Hz, 1H), 6.57 (s, 1H), 4.04 (s, 3H), 3.97 (s, 3H), 3.97 (s, 3H), 3.96 (s, 3H), 3.91 (s, 3H). ^{13}C NMR (126 MHz, CDCl_3) δ 177.80, 160.99, 151.86, 149.31, 144.13, 143.75, 143.40, 141.82, 126.01, 124.35, 119.56, 114.93, 111.17, 108.72, 107.33, 62.35, 61.61, 60.91, 56.10 \times 2. HR-MS (ESI) m/z Calcd. $\text{C}_{20}\text{H}_{22}\text{NO}^+$ $[\text{M}+\text{H}]^+$ 388.1391, Found 388.1391.

4.1.16. 2,3,4-Trimethoxyphenyl acetate (**20b**)

A mixture of **19b** (5.5 g, 30 mmol) and sodium acetate (4.9 g, 60 mmol) in acetic anhydride (28 mL, 300 mmol) was heated at 110 °C for 2 h. TLC analysis (petroleum ether/ethyl acetate = 9:1) showed completion of the reaction. Then the reaction mixture was concentrated under reduced pressure, diluted with water and extracted with ethyl acetate thrice. The organic phase was washed with brine, dried over anhydrous sodium sulfate. The organic layer was concentrated to afford product **20b** (6.4 g) as a brown yellow oil, which was used directly in the next step without further purification. Yield: 94%. ^1H NMR (500 MHz, CDCl_3) δ 6.74 (d, J = 9.0 Hz, 1H), 6.62 (d, J = 9.0 Hz, 1H), 3.89 (s, 3H), 3.88 (s, 3H), 3.85 (s, 3H), 2.31 (s, 3H).

4.1.17. 1-(2-Hydroxy-3,4-dimethoxyphenyl) ethan-1-one (**21a**)

A mixture of **19a** (1.5 g, 10 mmol) and sodium acetate (1.6 g, 20 mmol) in acetic anhydride (9.4 mL, 100 mmol) was heated at 110 °C for 2 h. TLC analysis (petroleum ether/ethyl acetate = 9:1) showed completion of the reaction. Then the reaction mixture was concentrated under reduced pressure, diluted with water and extracted with ethyl acetate thrice. The organic phase was washed with brine and dried over anhydrous sodium sulfate. The organic layer was concentrated to afford product **20a** (1.9 g) as a red brown oil, which was used directly in the next step without further purification. Then boron trifluoride etherate (ca. 48% BF_3 , 48.5 mL) was added dropwise to a solution of compound **20a** (1.9 g, 9.7 mmol) in glacial acetic acid (7.5 mL). The reaction mixture was stirred at 70 °C for 2 h. TLC analysis (petroleum ether/ethyl acetate = 7:3) showed completion of reaction. Then the reaction mixture was quenched with water and extracted with ethyl acetate. The organic phase was washed with brine, dried over anhydrous sodium sulfate, and purified by silica gel column chromatography (petroleum ether/ethyl acetate = 10:1) to afford product **21a** (1.8 g) as a brown solid. Yield: 95%. ^1H NMR (400 MHz, CDCl_3) δ 12.67 (s, 1H), 7.09 (s, 1H), 6.48 (s, 1H), 3.94 (s, 3H), 3.89 (s, 3H), 2.59 (s, 3H).

4.1.18. 1-(2-Hydroxy-3,4,5-trimethoxyphenyl) ethan-1-one (**21b**)

Boron trifluoride etherate (ca. 48% BF_3 , 140 mL) was added to a solution of **20b** (6.4 g, 28 mmol) in glacial acetic acid (21 mL). The reaction mixture was stirred at 70 °C for 2 h. TLC analysis (petroleum ether/ethyl acetate = 7:3) showed completion of reaction. Then the reaction mixture was quenched with water and extracted with ethyl acetate. The organic phase was washed with brine, dried over anhydrous sodium sulfate, and purified by silica gel column chromatography (petroleum ether/ethyl acetate = 10:1) to afford product **21b** (6.0 g) as a yellow solid. Yield: 95%. ^1H NMR (500 MHz, CDCl_3) δ 12.44 (s, 1H), 6.93 (s, 1H), 4.04 (s, 3H), 3.92 (s, 3H), 3.85 (s, 3H), 2.59 (s, 3H).

4.1.19. General procedure for synthesis of compounds **22a–22d**

To a solution of compound **21a–21d** (196 mg, 1.0 mmol) in dichloromethane (5 mL) was added triethylamine (418 μL , 3.0 mmol) and acyl chloride (1.5 mmol) at 0 °C. The mixture was stirred at rt for 2 h, then quenched with water and extracted with ethyl acetate. The organic phase was washed with brine, dried over anhydrous sodium sulfate, and purified by silica gel column chromatography (petroleum ether/ethyl acetate = 5:1) to afford the products **22a–22d** as white solids.

4.1.19.1. 6-Acetyl-2,3-dimethoxyphenyl 3,4-dimethoxybenzoate (**22a**). Yield: 78%. ^1H NMR (400 MHz, CDCl_3) δ 7.90 (dd, J = 8.4, 2.0 Hz, 1H), 7.69 (d, J = 1.8 Hz, 1H), 7.44 (s, 1H), 6.99 (d, J = 8.5 Hz, 1H), 6.69 (s, 1H), 3.99 (s, 3H), 3.97 (s, 3H), 3.93 (s, 3H), 2.51 (s, 3H).

4.1.19.2. 6-Acetyl-2,3-dimethoxyphenyl 3-methoxybenzoate (**22b**). Yield: 82%. ^1H NMR (400 MHz, CDCl_3) δ 7.83 (d, J = 7.7 Hz, 1H), 7.72 (s, 1H), 7.48–7.41 (m, 2H), 7.21 (dd, J = 8.3, 2.7 Hz, 1H), 6.68 (s, 1H), 3.95 (s, 3H), 3.93 (s, 3H), 3.89 (s, 3H), 2.51 (s, 3H).

4.1.19.3. 6-Acetyl-2,3-dimethoxyphenyl 4-methoxybenzoate (**22c**). Yield: 82%. ^1H NMR (400 MHz, CDCl_3) δ 8.18 (d, J = 8.8 Hz, 2H), 7.44 (s, 1H), 7.02 (d, J = 8.8 Hz, 2H), 6.67 (s, 1H), 3.95 (s, 3H), 3.92 (s, 3H), 3.91 (s, 3H), 2.50 (s, 3H).

4.1.19.4. 6-Acetyl-2,3,4-trimethoxyphenyl 3,4-dimethoxybenzoate (**22d**). Yield: 82%. ^1H NMR (400 MHz, CDCl_3) δ 7.93 (dd, J = 8.4, 1.9 Hz, 1H), 7.72 (d, J = 1.9 Hz, 1H), 7.23 (s, 1H), 7.00 (d, J = 8.5 Hz, 1H), 4.01 (s, 3H), 3.99 (s, 3H), 3.99 (s, 3H), 3.94 (s, 3H), 3.87 (s, 3H), 2.53 (s, 3H).

4.1.20. General procedure for synthesis of compounds **23a–23d**

To a solution of **22** (0.8 mmol) in dichloroethane (4.8 mL) was added triethylamine (332 μL , 2.4 mmol) and trimethylsilyl trifluoromethanesulfonate (868 μL , 4.8 mmol). The mixture was stirred at 95 °C for 2 h, then quenched with CH_3OH and extracted with ethyl acetate. The organic phase was washed with brine, dried over anhydrous sodium sulfate, and purified by silica gel column chromatography (petroleum ether/ethyl acetate = 2:1) to afford the products **23a–23d**.

4.1.20.1. 2-(3,4-Dimethoxyphenyl)-7,8-dimethoxy-4H-chromen-4-one (**23a**). Light yellow solid. Yield: 82%. Purity: 99%. ^1H NMR (400 MHz, CDCl_3) δ 7.57 (s, 1H), 7.54 (dd, J = 8.5, 1.8 Hz, 1H), 7.37 (d, J = 1.8 Hz, 1H), 6.98 (d, J = 9.3 Hz, 2H), 6.73 (s, 1H), 4.03 (s, 3H), 3.99 (s, 6H), 3.97 (s, 3H). ^{13}C NMR (101 MHz, CDCl_3) δ 177.63, 162.83, 154.37, 152.21, 151.85, 149.29, 147.61, 124.49, 119.72, 117.29, 111.16, 108.73, 106.07, 104.45, 99.79, 56.51, 56.38, 56.12, 56.09. HR-MS (ESI) m/z Calcd. $\text{C}_{19}\text{H}_{19}\text{O}_6^+$ $[\text{M}+\text{H}]^+$ 343.1176, Found 343.1166.

4.1.20.2. 7,8-Dimethoxy-2-(3-methoxyphenyl)-4H-chromen-4-one (**23b**). Breen solid. Yield: 82%. Purity: 99%. ^1H NMR (400 MHz, CDCl_3) δ 7.58 (s, 1H), 7.50 (d, J = 7.8 Hz, 1H), 7.44 (dd, J = 9.0, 6.8 Hz, 2H), 7.08 (dd, J = 8.0, 2.3 Hz, 1H), 7.01 (s, 1H), 6.79 (s, 1H), 4.04 (s, 3H), 4.01 (s, 3H), 3.91 (s, 3H). ^{13}C NMR (101 MHz, CDCl_3) δ 177.66, 162.57, 160.01, 154.52, 152.30, 147.71, 133.31, 130.10, 118.53, 117.37, 116.88, 111.59, 107.32, 104.38, 99.81, 56.51, 56.39.

55.49. HR-MS (ESI) m/z Calcd. $C_{18}H_{17}O_5^+$ [M+H]⁺ 313.1071, Found 313.1072.

4.1.20.3. *7,8-Dimethoxy-2-(4-methoxyphenyl)-4H-chromen-4-one (23c)*. Brick red solid. Yield: 82%. Purity: 99%. ¹H NMR (500 MHz, CDCl₃) δ 7.86 (d, J = 8.8 Hz, 2H), 7.56 (s, 1H), 7.02 (d, J = 8.7 Hz, 2H), 6.99 (s, 1H), 6.71 (s, 1H), 4.02 (s, 3H), 3.99 (s, 3H), 3.89 (s, 3H). ¹³C NMR (126 MHz, CDCl₃) δ 177.68, 162.85, 162.18, 154.31, 152.20, 147.55, 127.76 × 2, 124.27, 117.28, 114.43 × 2, 105.76, 104.45, 99.76, 56.48, 56.39, 55.51. HR-MS (ESI) m/z Calcd. $C_{18}H_{17}O_5^+$ [M+H]⁺ 313.1071, Found 313.1067.

4.1.20.4. *2-(3,4-Dimethoxyphenyl)-6,7,8-trimethoxy-4H-chromen-4-one (23d)*. White solid. Yield: 83%. Purity: 96%. ¹H NMR (500 MHz, MeOD-*d*₄) δ 7.68 (d, J = 8.4 Hz, 1H), 7.56 (s, 1H), 7.36 (s, 1H), 7.13 (d, J = 8.5 Hz, 1H), 6.82 (s, 1H), 4.12 (s, 3H), 4.04 (s, 3H), 3.97 (s, 6H), 3.94 (s, 3H). ¹³C NMR (101 MHz, CDCl₃) δ 177.72, 162.82, 152.00, 151.16, 149.32, 147.38, 145.75, 142.03, 124.40, 119.79 × 2, 111.25, 108.69, 105.64, 100.08, 62.02, 61.52, 56.30, 56.11, 55.99. HR-MS (ESI) m/z Calcd. $C_{20}H_{21}O_7^+$ [M+H]⁺ 373.1282, Found 373.1275.

4.1.21. *1-(2,3,4,5-Tetramethoxyphenyl)-ethan-1-one (24)*

To a solution of **21b** (2.3 g, 10 mmol) in DMF was added potassium carbonate (2.1 g, 15 mmol) and iodomethane (679 μL, 11 mmol). The reaction mixture was stirred at rt for 1 h and then extracted with ethyl acetate. The organic phase was washed with brine, dried over anhydrous sodium sulfate, and concentrated to afford product **24** (2.3 g) as a brown yellow oil, which was used directly in the next step without further purification. Yield: 96%. ¹H NMR (500 MHz, CDCl₃) δ 7.07 (s, 1H), 3.96 (s, 3H), 3.92 (s, 3H), 3.92 (s, 3H), 3.86 (s, 3H), 2.64 (s, 3H).

4.1.22. *1-(2,3,4,5-Tetramethoxy-6-nitrophenyl) ethan-1-one (25)*

Nitric acid (ca. 70% HNO₃, 798 μL, 18 mmol) was added dropwise to **24** (2.2 g, 9.0 mmol) over 15 min at 0 °C. Then the reaction mixture was quenched with water and extracted with ethyl acetate. The organic phase was washed with brine, dried over anhydrous sodium sulfate, and purified by silica gel column chromatography (petroleum ether/ethyl acetate = 5:1) to afford product **25** (1.9 g) as a light yellow solid. Yield: 74%. ¹H NMR (400 MHz, CDCl₃) δ 4.00 (s, 3H), 3.97 (s, 3H), 3.95 (s, 3H), 3.88 (s, 3H), 2.59 (s, 3H).

4.1.23. *1-(2-Amino-3,4,5,6-tetramethoxyphenyl) ethan-1-one (26)*

To a solution of **25** (1.9 g, 6.7 mmol) in tetrahydrofuran (134 mL) was added Pd/C catalyst (285 mg, 15%) under an atmosphere of H₂ at 40 °C for 15 h. After cooling to rt, the mixture was filtered with diatomite and washed with ethyl acetate. The organic layer was evaporated under vacuum to afford a residue, which was purified by silica gel column chromatography (petroleum ether/ethyl acetate = 2:1) to yield product **26** (1.6 g) as a brown yellow oil. Yield: 95%. ¹H NMR (400 MHz, CDCl₃) δ 4.12 (s, 3H), 4.03 (s, 3H), 4.02 (s, 3H), 3.88 (s, 3H), 2.83 (s, 3H).

4.1.24. *N-(2-Acetyl-3,4,5,6-tetramethoxyphenyl)-3,4-dimethoxybenzamide (27)*

To a solution of **26** (570 mg, 2.2 mmol) in dichloromethane (11 mL) was added triethylamine (915 μL, 6.6 mmol) and 3,4-

dimethoxybenzoyl chloride (883 mg, 4.4 mmol) at 0 °C. The mixture was stirred at rt for 2 h, then quenched with water and extracted with ethyl acetate. The organic phase was washed with brine, dried over anhydrous sodium sulfate, and purified by silica gel column chromatography (petroleum ether/ethyl acetate = 5:1) to afford product **27** (738 mg) as a white solid. Yield: 80%. ¹H NMR (400 MHz, CDCl₃) δ 8.24 (s, 1H), 7.46 (d, J = 1.9 Hz, 1H), 7.44 (dd, J = 8.2, 2.1 Hz, 1H), 6.92 (d, J = 8.2 Hz, 1H), 3.97 (s, 3H), 3.95 (s, 3H), 3.95 (s, 3H), 3.93 (s, 3H), 3.90 (s, 3H), 3.84 (s, 3H), 2.65 (s, 3H).

4.1.25. *2-(3,4-Dimethoxyphenyl)-5,6,7,8-tetramethoxyquinolin-4(1H)-one (28)*

To a solution of **27** (738 mg, 1.8 mmol) in anhydrous tetrahydrofuran (60 mL) was added potassium *tert*-butoxide (606 mg, 5.4 mmol) under an atmosphere of Ar at 75 °C for 18 h. After cooled to rt, the solution was poured into water and acidified by addition of 2.0 mol/L aqueous HCl. The resulting solution was extracted with portion of ethyl acetate. The combined organic extracts were dried over anhydrous sodium sulfate and concentrated to give a crude, which was purified by silica gel column chromatography (petroleum ether/ethyl acetate = 3:1) to yield product **28** (592 mg) as a white solid. Yield: 82%. Purity: 99%. ¹H NMR (400 MHz, CDCl₃) δ 7.35 (d, J = 6.6 Hz, 2H), 7.02 (d, J = 8.9 Hz, 1H), 6.72 (s, 1H), 4.12 (s, 3H), 4.09 (s, 3H), 4.03 (s, 3H), 4.00 (s, 6H), 3.98 (s, 3H). ¹³C NMR (126 MHz, MeOD-*d*₄) δ 176.98, 151.67, 150.93, 149.56, 149.38, 147.53, 143.88, 137.77, 132.72, 125.99, 120.52, 114.51, 111.48, 110.73, 107.50, 61.46, 60.91, 60.88, 60.61, 55.25, 55.14. HR-MS (ESI) m/z Calcd. $C_{21}H_{24}NO_7^+$ [M+H]⁺ 402.1547, Found 402.1542.

4.1.26. *2-(3,4-Dimethoxyphenyl)-5,6,7,8-tetramethoxy-1-methylquinolin-4(1H)-one (29a)*

To a solution of **28** (80 mg, 0.2 mmol) in DMF was added potassium carbonate (41 mg, 0.3 mmol) and iodomethane (14 μL, 0.22 mmol). The reaction mixture was stirred at rt for 1 h and then extracted with ethyl acetate. The organic phase was washed with brine, dried over anhydrous sodium sulfate, and concentrated to give a crude, which was purified by silica gel column chromatography (petroleum ether/ethyl acetate = 3:1) to yield product **29a** (62 mg) as a light yellow oil. Yield: 75%. Purity: 99%. ¹H NMR (400 MHz, CDCl₃) δ 7.94 (d, J = 2.0 Hz, 1H), 7.65 (dd, J = 8.4, 2.0 Hz, 1H), 7.14 (s, 1H), 6.98 (d, J = 8.4 Hz, 1H), 4.20 (s, 3H), 4.13 (s, 3H), 4.11 (s, 3H), 4.04 (s, 3H), 4.01 (s, 3H), 3.96 (s, 3H), 3.91 (s, 3H). ¹³C NMR (126 MHz, CDCl₃) δ 163.70, 155.98, 150.38, 149.21, 148.14, 145.20, 144.52, 144.45, 142.28, 132.78, 119.75, 112.38, 110.83, 110.45, 97.27, 62.33, 62.21, 61.76 × 2, 56.01, 55.96 × 2. HR-MS (ESI) m/z Calcd. $C_{22}H_{26}NO_7^+$ [M+H]⁺ 416.1704, Found 416.1710.

4.1.27. *General procedure for synthesis of compounds 29b–29d*

To a solution of **28** (0.2 mmol) in anhydrous DMF (2.0 mL) was added sodium hydride (48 mg, 2.0 mmol). The mixture was stirred at 90 °C for 30 min and chloralkanes (0.6 mmol) was added. Then the reaction mixture was further stirred at 90 °C for 2 h. After cooled to rt, the solution was poured into water and acidified by the addition of 2.0 mol/L aqueous HCl. The resulting solution was extracted with portion of ethyl acetate. The combined organic extracts were washed with brine, dried over anhydrous sodium sulfate, and concentrated to give crude, which was purified by

silica gel column chromatography (petroleum ether/ethyl acetate = 3:1) to yield the oily products.

4.1.27.1. 2-(3,4-Dimethoxyphenyl)-5,6,7,8-tetramethoxy-1-propylquinolin-4(1H)-one (**29b**). A light yellow oil. Yield: 62%. Purity: 99%. ¹H NMR (400 MHz, MeOD-*d*₄) δ 7.89 (d, *J* = 2.1 Hz, 1H), 7.68 (dd, *J* = 8.4, 2.1 Hz, 1H), 7.24 (s, 1H), 7.06 (d, *J* = 8.4 Hz, 1H), 4.25 (t, *J* = 6.4 Hz, 2H), 4.11 (s, 3H), 4.06 (s, 3H), 3.97 (s, 3H), 3.96 (s, 3H), 3.90 (s, 3H), 3.88 (s, 3H), 2.01 (dd, *J* = 13.9, 6.5 Hz, 2H), 1.19 (t, *J* = 7.4 Hz, 3H). ¹³C NMR (126 MHz, CDCl₃) δ 167.39, 160.83, 154.56, 153.11, 152.03, 149.02, 148.70, 148.09, 145.85, 136.38, 124.05, 116.32, 115.07, 114.73, 102.11, 74.21, 65.30, 65.23, 64.67 × 2, 59.04, 58.99, 26.17, 13.65. HR-MS (ESI) *m/z* Calcd. C₂₄H₃₀NO₇⁺ [M+H]⁺ 444.2017, Found 444.2019.

4.1.27.2. 2-(3,4-Dimethoxyphenyl)-5,6,7,8-tetramethoxy-1-(2-methoxyethyl)-quinolin-4(1H)-one (**29c**). A light yellow oil. Yield: 70%. Purity: 99%. ¹H NMR (400 MHz, MeOD-*d*₄) δ 7.90 (d, *J* = 2.1 Hz, 1H), 7.71 (dd, *J* = 8.4, 2.1 Hz, 1H), 7.28 (s, 1H), 7.07 (d, *J* = 8.4 Hz, 1H), 4.43 (t, *J* = 4.4 Hz, 2H), 4.11 (s, 3H), 4.07 (s, 3H), 3.97 (s, 3H), 3.97 (s, 3H), 3.93 (t, *J* = 4.4 Hz, 2H), 3.91 (s, 3H), 3.89 (s, 3H), 3.49 (s, 3H). ¹³C NMR (126 MHz, CDCl₃) δ 167.05, 160.80, 154.60, 153.12, 152.10, 149.12, 148.63, 148.11, 145.86, 136.30, 124.09, 116.27, 115.08, 114.74, 102.22, 74.50, 71.91, 65.37, 65.32, 64.69, 64.67, 61.80, 59.05, 59.00. HR-MS (ESI) *m/z* Calcd. C₂₄H₃₀NO₈⁺ [M+H]⁺ 460.1966, Found 460.1966.

4.1.27.3. 2-(3,4-Dimethoxyphenyl)-1-(2-(dimethylamino)ethyl)-5,6,7,8-tetramethoxyquinolin-4(1H)-one (**29d**). A brown oil. Yield: 71%. Purity: 97.1%. ¹H NMR (500 MHz, MeOD-*d*₄) δ 7.94 (s, 1H), 7.74 (d, *J* = 8.4 Hz, 1H), 7.32 (s, 1H), 7.08 (d, *J* = 8.4 Hz, 1H), 4.44 (t, *J* = 5.6 Hz, 2H), 4.13 (s, 3H), 4.08 (s, 3H), 3.99 (s, 6H), 3.92 (s, 3H), 3.90 (s, 3H), 3.03 (t, *J* = 5.5 Hz, 2H), 2.48 (s, 6H). ¹³C NMR (126 MHz, MeOD-*d*₄) δ 162.92, 156.80, 150.69, 149.19, 148.18, 145.14, 144.69, 144.14, 141.93, 132.32, 120.17, 112.25, 111.13, 110.81, 98.38, 66.81, 61.39, 61.31, 60.73, 60.71, 57.46, 55.12, 55.06, 44.81 × 2. HR-MS (ESI) *m/z* Calcd. C₂₅H₃₃N₂O₇⁺ [M+H]⁺ 473.2282, Found 473.2286.

4.2. Molecular docking and simulation for P-gp and **29d**

The detailed methods for molecular docking and simulation are shown in Supporting Information Section 1.

4.3. Cell viability assay, colony formation assay and animal models

The detailed methods for cell viability assay, colony formation assay and animal models are shown in Supporting Information Section 2.

Acknowledgments

This work was supported by National Key R&D Program of China (2017YFB0202600), Macao Science and Technology Development Fund, Macao Special Administrative Region (003/2017/A1 to Ying Xie, China), National Natural Science Foundation of China (21572279, 21877134, 81602955 and 81703341), Guangdong Province Higher Vocational Colleges & Schools Pearl River Scholar Funded Scheme (2016, China).

Author contributions

Deyan Wu, Ying Xie, and Hai-Bin Luo designed the research. Senling Feng and Huifang Zhou carried out the experiments and performed data analysis. Deyan Wu, Dechong Zheng, Biao Qu, Ruiming Liu, Chen Zhang, and Zhe Li participated part of the experiments. Huifang Zhou, Ying Xie, and Hai-Bin Luo wrote the manuscript. Ying Xie and Hai-Bin Luo revised the manuscript. All of the authors have read and approved the final manuscript.

Conflicts of interest

The authors have no conflicts of interest to declare.

Appendix A. Supporting information

Supporting data to this article can be found online at <https://doi.org/10.1016/j.apsb.2019.07.007>.

References

- Bray F, Ferlay J, Soerjomataram I, Siegel RL, Torre LA, Jemal A. Global cancer statistics 2018: GLOBOCAN estimates of incidence and mortality worldwide for 36 cancers in 185 countries. *CA: Cancer J Clin* 2018;**68**:394–424.
- Alfarouk KO, Stock CM, Taylor S, Walsh M, Muddathir AK, Verduzco D, et al. Resistance to cancer chemotherapy: failure in drug response from ADME to P-gp. *Cancer Cell Int* 2015;**15**:71.
- Elshimali YI, Wu Y, Khaddour H, Wu Y, Gradinaru D, Sukhija H, et al. Optimization of cancer treatment through overcoming drug resistance. *J Cancer Res Oncobiol* 2018;**1**:107.
- Callaghan R, Luk F, Bebawy M. Inhibition of the multidrug resistance p-glycoprotein: time for a change of strategy?. *Drug Metab Dispos* 2014;**42**:623–31.
- Zhang H, Huang L, Tao L, Zhang J, Wang F, Zhang X, et al. Secalonic acid D induces cell apoptosis in both sensitive and ABCG2-overexpressing multidrug resistant cancer cells through upregulating c-Jun expression. *Acta Pharm Sin B* 2019;**9**:516–25.
- Chang L, Xiao M, Yang L, Wang S, Wang SQ, Bender A, et al. Discovery of a non-toxic [1,2,4]triazolo[1,5-*a*]pyrimidin-7-one (WS-10) that modulates ABCB1-mediated multidrug resistance (MDR). *Bioorg Med Chem* 2018;**26**:5974–85.
- Wen Y, Zhao R, Gupta P, Fan Y, Zhang Y, Huang Z, et al. The epigallocatechin gallate derivative Y₆ reverses drug resistance mediated by the ABCB1 transporter both *in vitro* and *in vivo*. *Acta Pharm Sin B* 2019;**9**:316–23.
- Zhang L, Zhang X, Zhang C, Bai X, Zhang J, Zhao X, et al. Nobiletin promotes antioxidant and anti-inflammatory responses and elicits protection against ischemic stroke *in vivo*. *Brain Res* 2016;**1636**:130–41.
- Murakami A, Nakamura Y, Torikai K, Tanaka T, Koshiba T, Koshimizu K, et al. Inhibitory effect of citrus nobiletin on phorbol ester-induced skin inflammation, oxidative stress, and tumor promotion in mice. *Cancer Res* 2000;**60**:5059–66.
- Ma W, Feng S, Yao X, Yuan Z, Liu L, Xie Y. Nobiletin enhances the efficacy of chemotherapeutic agents in ABCB1 overexpression cancer cells. *Sci Rep* 2015;**5**:18789.
- Onoue S, Nakamura T, Uchida A, Ogawa K, Yuminoki K, Hashimoto N, et al. Physicochemical and biopharmaceutical characterization of amorphous solid dispersion of nobiletin, a citrus polymethoxylated flavone, with improved hepatoprotective effects. *Eur J Pharm Sci* 2013;**49**:453–60.
- Asakawa T, Hiza A, Nakayama M, Inai M, Oyama D, Koide H, et al. PET Imaging of nobiletin based on a practical total synthesis. *Chem Commun* 2011;**47**:2868–70.

13. Guo Y, Ji SZ, Chen C, Liu HW, Zhao JH, Zheng YL, et al. A ligand-free, powerful, and practical method for methoxylation of unactivated aryl bromides by use of the CuCl/HCOOMe/MeONa/MeOH system. *Res Chem Intermed* 2015;**41**:8651–64.
14. Yoshida M, Saito K, Fujino Y, Doi T. A concise synthesis of 3-aroylflavones via lewis base 9-azajulolidine-catalyzed tandem acyl transfer-cyclization. *Chem Commun* 2012;**48**:11796–8.
15. Rocha DH, Pinto DC, Silva AM. Synthesis and cyclisation studies of (*E*)-2-Aryl-1-methyl-3-styrylquinolin-4(1*H*)-ones. *Tetrahedron* 2015;**71**:7717–21.
16. Wesolowska O, Wiśniewski J, Środa-Pomianek K, Bielawska-Pohl A, Paprocka M, Duś D, et al. Multidrug resistance reversal and apoptosis induction in human colon cancer cells by some flavonoids present in *Citrus* plants. *J Nat Prod* 2012;**75**:1896–902.
17. Martins IL, Charneira C, Gandin V, Da Silva JL, Justino GC, Telo JP, et al. Selenium-containing chrysin and quercetin derivatives: attractive scaffolds for cancer therapy. *J Med Chem* 2015;**58**:4250–65.
18. Hadjeri M, Barbier M, Ronot X, Mariotte AM, Boumendjel A, Boutonnat J. Modulation of P-glycoprotein-mediated multidrug resistance by flavonoid derivatives and analogues. *J Med Chem* 2003;**46**:2125–31.
19. Vassileva V, Grant J, De Souza R, Allen C, Piquette-Miller M. Novel biocompatible intraperitoneal drug delivery system increases tolerability and therapeutic efficacy of paclitaxel in a human ovarian cancer xenograft model. *Cancer Chemother Pharmacol* 2007;**60**:907–14.
20. De Oliveira Júnior RG, Christiane Adrielly AF, Da Silva Almeida JR, Grougnet R, Thiéry V, Picot L. Sensitization of tumor cells to chemotherapy by natural products: a systematic review of preclinical data and molecular mechanisms. *Fitoterapia* 2018;**129**:383–400.
21. Huang H, Li L, Shi W, Liu H, Yang J, Yuan X, et al. The multi-functional effects of nobiletin and its metabolites *in vivo* and *in vitro*. *Evid Based Complement Alternat Med* 2016;**2016**:2918796.
22. Wu X, Song M, Rakariyatham K, Zheng J, Wang M, Xu F, et al. Inhibitory effects of 4'-demethylnobiletin, a metabolite of nobiletin, on 12-*O*-tetradecanoylphorbol-13-acetate (TPA)-induced inflammation in mouse ears. *J Agric Food Chem* 2015;**63**:10921–7.